

The Design and Performance of Scintillator/Cherenkov Fiber Forward Calorimeter for GEM

Robert C. Webb
Texas A&M University

October 2, 1992

Abstract:

The kinematic region beyond $\eta = 3$ at the Superconducting Super Collider (SSC) provide some special challenges for high performance calorimetry. In this region, hadron showers cover rather large regions η of and radiation levels beyond $\eta = 5.5$ near the beam pipe can exceed 10^9 Rads per standard SSC year at luminosities of $10^{34} \text{ cm}^{-2} \text{ sec}^{-1}$. However in order to access the physics processes with missing E_T signatures, this kinematic region is of extreme importance.

In the note which follows, we will describe the design and performance of a fast, projective, rad hard scintillator/quartz fiber sampling calorimeter for the forward regions in the GEM experiment. This calorimeter should provide the energy and spatial resolution required for this missing E_T physics while being robust enough to survive ten years of operation at a nominal luminosity of 10^{33} .

D R A F T

The Design and Performance of Scintillator/Cherenkov Fiber Forward Calorimeter for GEM

Robert C. Webb
Texas A&M University

Abstract

The kinematic region beyond $\eta = 3$ at the Superconducting Super Collider (SSC) provide some special challenges for high performance calorimetry. In this region, hadron showers cover rather large regions of η and radiation levels beyond $\eta = 5.5$ near the beam pipe can exceed 10^9 Rads per standard SSC year at luminosities of 10^{34} cm^{-2} sec^{-1} . However in order to access the physics processes with missing E_T signatures, this kinematic region is of extreme importance.

In the note which follows, we will describe the design and performance of a fast, projective, rad hard scintillator/quartz fiber sampling calorimeter for the forward regions in the GEM experiment. This calorimeter should provide the energy and spatial resolution required for this missing E_T physics while being robust enough to survive ten years of operation at a nominal luminosity of 10^{33} .

I. Introduction

The "spaghetti calorimeter" concept for high quality and high performance electromagnetic and hadronic calorimetry has made significant advances through the efforts of the SPACAL and SSCintCAL R&D programs both here and abroad. The spaghetti calorimeter based on solid scintillating fibers has been shown to have high resolution, fast response and radiation survivability for $\eta \leq 3$ all at a relatively modest cost (eg. The JETSET^[1] group has shown that it is possible to achieve energy resolutions for *em* showers of $7\%/\sqrt{E}$ with a 50% by volume mix of fibers and lead absorber; The SPACAL group has demonstrated the possibility of doing electron/hadron id using the temporal response of these calorimeters^[2]; and Kuraray and Bicron have developed new rad hard fibers using 3HF which can withstand doses of at least 10 MRad without significant changes in fiber response^[3]). The SSCintCAL group working with the GEM R&D program have taken these developments and designed a compact, relatively low cost hadron calorimeter for the GEM experiment to cover the angular ranges from $\eta = 0$ to $\eta = 3.0$ ^[4]. Given that the spaghetti calorimeter concept using solid scintillating fibers is the most

cost effective/high performance hadron calorimeter choice for GEM, we have been studying the possibility of finding a rad hard equivalent of this technology to be used in conjunction with spaghetti calorimetry for $\eta > 3$.

This R&D has led to the development of three solutions to this forward calorimeter design problem. All three of these solutions use the principal of total internal reflection(TIR) for light propagation coupled with either scintillation or cherenkov light being produced by *em*/hadron showers in the fiber/capillary core material. For the scintillating solution [5], we have developed both a flexible and rigid capillary design where the capillaries are filled with a rad hard scintillating liquid and embedded in an absorber matrix. The TIR coating materials are chosen for their radiation hardness and chemical inertness, as well as their indices of refraction (see Table I); and the scintillators being investigated are known to be insensitive to radiation doses at the level of 100 MRad [6]. The third concept that we have been pursuing is one which is based on the principal of sampling cherenkov calorimeters (e.g. lead glass) where the actual media is a high purity quartz fiber. Pure quartz is also known to be extremely rad hard [7] at the level of at least 1 GRad and these fibers can be coated either with a rad hard TIR film or they may be left unclad taking advantage of an air gap to make an extremely robust sampling calorimeter media.

The concept described here for the GEM forward calorimeter is relatively insensitive to the particular choice of active media used in the final calorimeter. We have engineered this system to allow for using the most robust of the three technologies available once the R&D program has been completed. For the sake of completeness, we will present the details of all of these technologies as we know them. However, at this time it appears that based on the extreme rad hardness of the quartz fiber technology, this technically is the current *front runner* in our consideration.

II. The FCAL Design

For the GEM experimental configuration, we have designed a compact forward calorimeter (FCAL) that mates with the scintillating calorimeter at $\eta = 3$ and covers the forward region down to the beam pipe at a distance of 3.73 m from the IR. This design produces a very compact hadron calorimeter configuration from $\eta = 0$ to $\eta = 5.5$ with no " $\eta = 3$ " problem like that seen in calorimeters like those used in D0 and proposed in EMPACT. This compact design provides the optimal shielding configuration for the GEM muon system within the space available. However, the final z position of the front face of this system can be adjusted to balance muon shielding issues with missing E_T issues.

a. Absorber

In order to keep the shower sizes relatively compact we have opted to use tungsten as the absorber of choice for this exercise ($\lambda_a = 11$ cm). We are also investigating the possibility of using alternative absorbers of either copper ($\lambda_a = 15$

cm) or a lead eutectic/tungsten shot mixture ($\lambda_a = 15$ cm) in place of the tungsten absorber.

In the case of the tungsten solution, the calorimeter will be fabricated out of tungsten pellets that can be stacked in a form to build a projective tower [8]. The sampling fraction for this calorimeter can be tailored for the particular choice of active media by adjusting the size of the pellets used. For the scintillator option we have designed a configuration with an absorber to active media ratio of 4:1. For the quartz fiber version, the packing fraction would be altered to 9:1 or so to provide for compensation. The detail design of these tungsten pellets has been studied by the Oak Ridge Mechanical Engineering Group [8]. Figure 1 shows the profile of one of these tungsten pellets. Figure 2 shows the hole pattern that can be built up through the stacking of the pellets for the 4:1 packing fraction.

For the case in which we are using the quartz fibers as an active media, these fibers would be inserted into the matrix after the tungsten has been stacked and the fibers would then be bundled and brought to the surface of a quartz windowed, magnetic field insensitive photomultiplier tube. The phototubes at the back of the calorimeter have been positioned as far from the beam pipe as is practical to keep the radiation field in the vicinity of these photodetectors as low as possible (See Figure 3 for details). For the liquid spaghetti version of this system, each super tower would be lined with capillaries and a liquid distribution system would be built into the mechanical structure holding the tower together. Light from these capillaries would be brought out of the detector volume on quartz fiber light guides and the rest of the mechanics would be the same as that for the quartz FCAL.

The calorimeter will be made in mechanical modules which will contain four or more readout towers in η, ϕ space. The η, ϕ segmentation is varied to match shower size more closely to the bin size in this region. Figure 4 shows the η, ϕ layout of the towers in one of the FCAL systems. The FCAL system contains ~ 500 towers per side in the current design and covers an eta range from $\eta = 3$ to $\eta = 5.5$ at the beam pipe. Table II shows the physical boundaries for the mechanical super towers.

b. Z-Position

One other aspect of the FCAL that needs eventually to be optimized is its z position relative to the IR. The choice of this location presents us with a trade off between better angular resolution and lower radiation fluxes in the calorimeter at large z to poorer resolution and higher radiation fields but lower neutron fluxes in the muon system following the FCAL at positions closer to the IR. At this time we have opted for the more conservative approach regarding the neutron backgrounds in the muon system and have brought the FCAL in as close as is possible. To further shield the muon system from these neutrons, we have extended the last tower in the end wall calorimeter, whose boundary meets the $\eta = 3$ line, to extend to the rear face of the FCAL. This configuration should produce the best situation for the muon system.

It has been pointed out that all other hadron collider experiments have opted for a forward calorimeter that is far from the IR. This choice stems from the following consideration. If one is to choose a "close in" configuration, the calorimeter must plug the hole in the end wall calorimeter to give hermetic calorimeter coverage and provide adequate shielding for the following muon system. On the other hand, if you wish to consider the "far" configuration, the FCAL must be outside the main spectrometer volume so as not to produce neutron and albedo backgrounds in the external muon systems. If you find yourself anywhere in between these two limits, you run the risk of seriously spoiling the muon system performance.

It is also worth noting that the Liquid Argon version of the FCAL ends up further from the IR due to the space taken up by the Liquid Argon End Wall Calorimeter. It is possible that by adjusting the length of this boundary tower we can move the FCAL further from the IR while keeping the neutron fluxes in the muon system at a manageable level. Eventually this position choice will need to be revisited to optimize the FCAL location, however for the purposes of this discussion, we will consider it to be located at $z = 3.73$ m.

c. Projectivity

The calorimeter configuration currently under consideration is projective with the fibers within the absorber matrix oriented along the central ray of the mechanical tower. For the quartz fiber version of the FCAL, the expected performance of the calorimeter is relatively insensitive to the orientation of the fibers. Figure 5 from the work of Ph. Gorodetzky and Figure 6 from the work of E. Tarkovsky at Oak Ridge shows that channeling effects for the quartz fiber FCAL are small. For the liquid scintillation version, however, these projective capillaries can lead to spatial nonuniformities in response. Hence, to deal with this potential difficulty, we would propose placing several radiation lengths of material in front of the active volume of the calorimeter to begin spreading out the em cores of these showers. The performance of such a scintillator FCAL needs to be studied further through a simulation should we decide to pursue this technology.

d. Longitudinal Segmentation

The spaghetti calorimeter concept does not naturally lend itself to longitudinal segmentation. However, as a consequence of the projective nature of the FCAL design being proposed, there is a lateral segmentation built in. In previous studies on BaF_2 calorimetry using shower shape analysis ^[9] and from the work of the SPACAL collaboration ^[10], it seems possible that this lateral segmentation can be used for separating em from hadronic showers and thereby providing "effective" longitudinal segmentation. In the FCAL design being considered, the capillary/fibers which originate on the front face and traverse the entire length of the module will be read out by a separate photomultiplier from those fibers whose starting point is located somewhere on the side faces of a tower. By choosing the $\eta\phi$ segmentation for the front face of the scintillating option appropriately, we can

optimize out jet angular resolution measure.

e. Active Media Choice

One feature of this configuration which is not completely understood at this time is the effect of choosing quartz fibers as the active element versus the liquid scintillator filled capillaries regarding the usefulness of the transverse segmentation. The transverse shower shape of a hadronic shower is well understood for spaghetti style calorimeters (see Figure 7), but the usefulness of this transverse shower information for cherenkov style sampling calorimeters is not clear. For the cherenkov calorimeters, the detecting media is sensitive only to the relativistic particles within the shower and hence may sample quite a different profile. Simple arguments based on the simulation work of Gorodetzky and Tarkovsky showing little "channeling" down the fiber and "good" acceptance for large angle fast electrons would indicate that the quartz fiber calorimeter will likely sample only the core of a hadron shower and therefore be very collimated. It is clear that to really answer this question satisfactorily will require the completion of the simulation work underway, however at this time this does not appear to be a show stopper.

f. Rad-Hardness

One of the most critical items which we must discuss here is the plan for making the FCAL robust enough to survive the harsh radiation environment present in this kinematic region. For either of the FCAL versions being described in this document, this is an important element of the design concept. For the quartz fiber version, there is evidence [11] that such a calorimeter can withstand GRads of dose without seriously effecting its performance. In fact, in these tests the supporting material disintegrated causing an end to the tests. In this case, we would monitor the calibration of this system using physics signals and calibration system. When the performance had degraded beyond the safety zone allowed, we would remove the damaged fibers and replace them with new ones. We would imagine that this would happen on the time scale of every 3 - 5 yrs. even at the highest luminosities planned.

For the liquid version of the FCAL the system is quite different. Here we envision that we will have a liquid recirculating system for the scintillation fluid in this detector. While every effort would be made to choose the most rad hard scintillator for this purpose (survival of dose rate in the range of 10 - 100 MRad)^[6] the liquid would be continuously monitored and filtered outside the forward region's radiation field. When the performance of the liquid scintillator ranges outside the allowed operating zone, we would then drain and refill the system with fresh scintillator.

g. Compensation

Lastly, the issue of compensation of such an FCAL must be addressed. The two solutions being proposed have vastly different behaviors in this region. For

the liquid scintillator version, we are able to adjust the sampling fraction such that the calorimeter is nearly compensating $e/\pi \sim 1.0$. For a lead absorber the appropriate ratio is 4:1, however, the correct ratio for tungsten is probably from 5 or 6 to 1. The sampling fraction would be adjusted to bring this quantity to near 1.0 for this version of the FCAL. For the quartz fiber version of the FCAL, we expect the e/π ratio to be significantly greater than unity due to the blindness of the active material to the lower energy components of the hadronic showers. We can address part of the problem in this configuration by reducing the fiber fraction to 10% or less, however, eventually we may have to live with an e/h of 1.5. The effect of this non compensation will be to add a constant term to our jet energy resolution. At this time we have not done enough careful simulation of this style of calorimeter to determine whether the addition of this constant term will be large enough to degrade significantly the performance of this detector.

III. Material Studies for the GEM FCAL

As mentioned earlier, the forward regions at the SSC place serious constraints on the FCAL's ability to survive for long periods of operation (1 - 2 yrs.) without major access. In addition, the optical characteristics required for successful operation of the spaghetti versions of the FCAL also bring to light questions concerning the effect of radiation on these materials long before they are noticeably damaged mechanically. The R&D program for the FCAL development has focussed a substantial fraction of its effort in investigating these issues. While this has been one of the high priority elements of the R&D program, it is important to note that due to the relatively small amount of money being made available for this work, there are still many aspects of this that require study before we can make our final design choices. In this section we will summarize what has been learned thus far and what questions remain to be investigated.

a. Rad-hardness Studies

The main issue for either the liquid scintillator or the quartz fiber versions of the FCAL is that of survivability in the face of very high radiation doses $> \text{MRad/yr}$ even at luminosities of 10^{33} . Many materials when subjected to doses of ionizing radiation and neutrons at those levels suffer mechanical and radiochemical damage to such a large enough extent that they are inappropriate for use in this region of phase space. Unfortunately many standard materials used in conventional high energy physics experiments fall into this category. As a result our efforts have been aimed at locating suitable rad hard replacement materials for these less robust ones. Table I shows the effects of radiation damage on several of these materials. From this table one can see that there do exist some materials which in principal can survive in the environment. The challenge that we face has been to see if these materials or materials similar in rad hardness can be processed for use in building this GEM FCAL. The difficulty of this effort has been compounded by the fact that for the "optical based" solutions we are presenting here,

these materials not only must be rad hard, but they also must have extremely high optical quality in order for them to perform adequately in the FCAL.

In the quartz fiber FCAL, the issue of radiation hardness looks to be in the best shape. It is well known that pure quartz can withstand large radiation doses without being seriously damaged either optically or mechanically [12]. Based on this observation, the idea of building a quartz fiber cherenkov calorimeter has already been investigated at CERN. In work presented to the GEM calorimetry group in May, 1992 by Phillippe Gorodetzky, we have seen that a quartz calorimeter has been given a dose of ~ 10 GRad without serious degradation in its response. At these dose levels, the bulk quartz material remains relatively transparent in the wave length range of 2000 - 5000 Å (See Figure 8). While these dose levels do not effect the bulk quartz properties, they are observed to seriously effect the typical coating materials used on these fibers. At this time it is not fully understood whether this mechanical degradation of the coating has a serious effect on the optical properties of the fibers, since the TIR mechanism for light propagation is not used at all on the mechanical properties, but on the optical properties of the coating material and the boundary interface region. We are currently investigating this aspect of the quartz fiber system with experts in this area from Lawrence Livermore. It appears from their experience that several possible solutions to this problem do exist. Before a definitive answer can be given on this, further R&D study will need to be carried out.

In the case of the liquid scintillator version of the FCAL, we have made preliminary studies on the mineral oil based scintillator that we have been evaluating for this application. Those studies [13] have shown us that at the 10 MRad dose level the optical properties of this mineral oil based liquid remain relatively unchanged. We did observe some subtle changes in light output and optical attenuation lengths in these studies, however at this time we are not certain whether these changes were due to the radiation dose or to other forms of contamination which seem to effect the properties of this scintillating mixture similarly. Figures 9a and b show some of the previous work on radiation hard liquids.

In addition work performed by the group working on FCAL R&D in the SDC group have identified high index liquids which have survived doses in excess of 100 MRad without any noticeable degradation in response. Due to the limited resources and manpower available for these studies we have opted for studying the issue of producing suitable TIR capillaries at this time and plan to return to the study of these radiation effects once the optimal configuration has been formulated. At this time there are at least two solutions providing survivability at a 10 MRad dose, and we expect with further R&D this could be improved further.

b. Optical Properties

In addition to the stringent requirements on radiation survivability, the optical properties of the sampling media are critical to the successful operation and performance of the FCAL system. Here is where the bulk of our R&D efforts have

been focussed over the past two years. We have been studying ways of producing acceptable capillaries for use in this system which are potentially radiation hard, have the appropriate range of indices of refraction and can be produced at an affordable cost.

For the case of the quartz fiber solution, we have investigated the acquisition of obtaining high purity quartz optical fibers with and without cladding for use in the FCAL. The optics of the combination of TIR and cherenkov radiation place some restrictions on the orientation of the fibers for various core cladding systems. For bare fibers the propagation of cherenkov light down the fibers has a very large region of angle and impact parameter space where the light yield is high. This would provide the best situation for a sampling calorimeter in terms of light yield. Unfortunately, the cladding on these fibers interact with the effective propagation of the cherenkov light in more ways than simply changing the numerical aperture of the fiber. The optical quality of the surface of a clad fiber appears to yield better light propagation than that of an unclad fiber at this time. We do not completely understand the interplay between these claddings, the numerical aperture of the fiber and the overall light yield of a quartz fiber FCAL. The unclad fibers are typically processed differently and with poorer quality control than the clad fibers so this is an extra added dimension in this problem. All that we can conclude at this time is that there appears to be a broad range of fiber orientations (including 0°) which could be utilized effectively in a quartz FCAL. It is clear that a serious R&D effort studying the effects of surface quality and cladding material on calorimeter operation must be undertaken to answer these open questions as well as a more complete calorimeter simulation to determine the optical configuration of the active media.

For the case of the liquid filled capillaries, we have gained a significant experience in providing appropriate coating substances for use in these calorimeters. The R&D effort at TAMU has studied the quality of optical surfaces and light propagation down 1 - 3 mm diameter capillaries as a function of substrate material and their finish. We have concentrated our efforts on studying coating, materials (capillaries with known high radiation resistance (eg. PEEK, Kapton/Polyimides, Halar/ECTFE, PUR/ether polyurethane, Viton, Silicone, Tefzel/ECTFE, TeflonAF, polymethylsiloxane/PDMS; to name a few). In our work on depositing PDMS on glass or stainless steel substrates we have been able to achieve light propagation attenuation lengths in the 2 m range for high quality surface finishes on the substrate. Our measurements show that the optical properties depend on both bulk and surface properties of these capillaries. We can characterize the optical transmission down the length of one of these capillaries by the expression

$$I(z) = I(0)e^{-z/\lambda_{eff}}$$

where z is the length of transport down the fiber and λ_{eff} is the effective

length of the fiber with

$$\frac{1}{\lambda_{eff}} = \frac{1}{\lambda_{bulk}} + \frac{1}{\lambda_{surface}}.$$

In our studies of both liquid filled and quartz capillaries we have been able to isolate these two effects. For the liquid filled capillaries we have achieved $\lambda_{eff} \sim 2.00$ m with $\lambda_{bulk} \cong 20.00$ m and $\lambda_{surface} \cong 2.00$ m (See Figure 10). More routinely we have found that typical $\lambda_{surface}$ for the substrates under investigation give $\lambda_{surface} \sim 1.00$ m. Still a bit too short for the FCAL design contemplated. For λ_{eff} in the 2.0 m range for a 2 mm, this corresponds to a TIR reflection coefficient for a single bounce of approximately .999, while specular reflection along this same capillary would yield a λ_{eff} of ~ 6 cm!! We plan to continue R&D of this sort to develop a more routine technique for producing capillaries with $\lambda_{surface} \geq 2.00$ m.

Our studies of unclad quartz fibers have also yielded some results on these two absorption coefficients. Nominally for ultra pure quartz, $\lambda_{bulk} \sim 10$ m or so (see Figure 11). From our measurements of a small number of unpolished quartz rod, 2 mm in diameter we have measured a $\lambda_{surface} \sim .65 - .94$ m (see Figure 12). We understand this to be largely due to the non uniformity of the rod cross section and the effects of surface oils and dirt which act to reduce $\lambda_{surface}$ significantly. We expect that by taking similar care in producing unclad quartz rod as that used in fabricating clad fibers where $\lambda_{surface} \sim 2 - 10$ m, we should be able to produce unclad fiber with appropriate transmission properties.

IV. Expected Performance and Simulation

The energy and position resolution required by a suitable FCAL have been previously outlined in GEM TN - 92 - 70. In this document it was noted that in order to carry out the missing E_T program mentioned earlier a $\sigma E_T/E_T \leq 10\%$. These performance parameters have been included in the GEM baseline performance for the FCAL.

The expected performance for the liquid scintillator FCAL closely parallels that of the central and end wall spaghetti hadron calorimeter described elsewhere. Since the packing fraction of fibers is comparable to that in the central hadron system and the light output of the liquid filled capillaries is of the same order of magnitude as that observed from solid fibers, we expect the energy resolution of the scintillator FCAL to easily achieve $100\%/\sqrt{E}$. We base this on the observed resolution of the SSCintCAL modules recently studied in the BNL test beam and simulation work carried out by J. White and colleagues [6] for the SDC FCAL design. Table III shows the results of their GEANT studies of the stochastic terms sensitivity to the capillary attenuation length. This table shows that as long as $\lambda_{eff} > 2$ m the required energy resolution will be achievable.

The spatial resolution issue is at this time less well understood. In the forward region, position resolution significantly influences $\sigma E_T/E_T$ resolution. This

E_T resolution depends upon four major elements, the calorimeter energy resolution, the shower size, the calorimeter segmentation and the calorimeter position. The studies described in GEM TN-91- XX on the liquid argon FCAL indicate that it is possible to achieve $\sigma E_T/E_T < 10\%$ goal, however the corresponding detailed simulation studies for the scintillation/quartz option option have yet to be completed. The primary issue for the spatial resolution is not how finely the segmentation can be made, but the matching of the segmentation to the shower core size. For any of the techniques being considered, including the liquid argon concept, we must tailor our $\eta\phi$ segmentation in order to be able to do a shower shape analysis. This analysis can be done successfully to the few mm level when the segmentation is one third or less the shower core size [14]. This is clearly an area which must be better understood for all technologies before making a final technology choice.

The quartz fiber FCAL on the other hand does not closely parallel the performance of the spaghetti calorimeters, hence we must draw upon the work done at CERN with these type of calorimeters to predict the response of the quartz FCAL. Based on the CERN work and recent BNL test beam results for the SSCintCAL collaboration, we expect to measure a hadronic energy resolution of $213\%/\sqrt{E}$ where the resolution is being dominated by the photon statistics of the light collected, see Figure 13. This is a bit above what has been targeted as our performance goal in the baseline document however, the critical issue is what is the $\sigma E_T/E_T$ for this configuration? Here once again, the results are strongly dependent on the same factors mentioned in the discussion on the liquid scintillation system. For the quartz fiber case however, we expect that the observed shower profile may be more heavily collimated than a typical hadron shower due to the cherenkov sampling. If this effect can be seen, demonstrated through Monte Carlo simulations, this better position information could counteract the poorer energy resolution and provide for adequate missing E_T resolution. In this simulation area we are a bit better off, since a significant simulation effort is now gearing up at BU [15], ORNL [16] and SSCL to address this and several other important issues relating to the quartz fiber option.

V. Test Beam Results

During the recent summer test beam program at BNL the SSCintCAL group had the opportunity to study several different prototype calorimeters. Among these prototype studies was the testing of three different versions of prototype calorimeters using the technologies we have presented here for use in the GEM FCAL. The three devices tested were 1) fixed liquid filled capillary module (TAMU) 2) a removable, flexible, liquid filled capillary module (Fairfield) and 3) a quartz fiber module (Fairfield). We will summarize here the results of these beam tests.

Due to time constraints and the heavy load of other test beam activities in the A3 beamline during this time frame, the measurements on these prototype

modules were limited. We were able to study each using a single energy electron beam and for the case of the two Fairfield units parasitic muon data was also taken. Given the limited availability of beam, many of the important questions which arise concerning technologies of the kind (eg. uniformity of response, response as a function of incident beam angle, linearity of response versus energy to name a few) were not studied. Despite the limited tests carried out on these modules, the performance of these devices appeared to meet our expectations and demonstrated the viability of these technologies for choice in the FCAL system.

a. Fixed Capillary Results

The *em* prototype tested here was built by the TAMU group in order to make some general tests of this liquid filled capillary concept. The capillary walls were constructed with 1 mm diameter Teflon tubing, known not to be rad hard, but readily available with the right index of refraction for such an application. These capillaries were filled with a low index of refraction ($n = 1.47$) light mineral oil based scintillator which was chosen for its long bulk attenuation length properties. The capillaries were embedded in a lead matrix made from machined lead plates. These capillaries were arranged in a hexagonal pattern with the capillary to absorber volume ratio of 1:4 and fabricated into hexagonal modules of length 8.2 in and dimension across the face of ~ 2 in apex to apex. The details of the hole pattern is shown in Figure 14. The scintillation light is transported out of the absorber block using plastic optical fibers. These fibers are then glued to the face of a hexagonal light mixer and the light is transported down the mixer to the face of the detecting photomultiplier. The assembly of one of these *em* modules is presented in Figure 15. Seven such modules were constructed using the Teflon tubing to build a hexagonal array with a diameter of ~ 6 in (see Figure 16). This group of seven modules was studied using cosmic rays and in the BNL test beam.

Using a cosmic ray telescope we studied the response of this group of seven modules to minimum ionizing particles. These studies were undertaken with the cosmic ray muons traveling both parallel and perpendicular to the long axes of these modules. In the data taken with the muons travelling perpendicular to the module axis we observed a total light output for the seven modules of 12 *pe* for a particle crossing the diameter of this array. Converting this to an equivalent *pe/GeV* we have measured approximately 50 *pe/GeV* in this configuration. (see Figure 17)

In the test beam due to space and time constraints we were able only to study the collection of modules at one electron energy and with the array axis perpendicular to the beam direction. The average pulse heights measured in each of the seven blocks is shown in Figure 18 and the total energy sum is shown in Figure 19. This scintillation module shows an average light yield of 1200 *pe* for a 10 GeV electron and a relative energy resolution of 15%. We expect that with larger diameter capillaries with better optical properties than in the prototype that we should be able to reach *em* resolutions in the range of 10% at 10 GeV.

The performance for these modules were as follows:

$$\begin{aligned}\sigma/E &= 15\% \text{ for electrons @ 10 GeV} \\ 120 \text{ pe/GeV} &\text{ for electrons @ 10 GeV.}\end{aligned}$$

b. Flexible Capillary/Quartz Result

The Fairfield University team also staged a test of the prototype *em* calorimeter for which it was possible to change out the sampling media from flexible sealed scintillation filled capillaries to quartz fibers. The module was essentially a stack of square lead pieces 12.8 mm on a side and ~ 1.2 cm thick. Fifteen such plates were stacked to form the module. In each plate a square array of 3 mm diameter holes were drilled on a .92 cm spacing. Figure 20a shows hole pattern and Figure 20b the assembled lead stack. The read out of light from this module was accomplished by bundling the capillaries/quartz fibers and placing the end face of the bundle in contact with the phototube face. A single phototube was used in these tests (see Figure 20b).

For the data taken using the liquid scintillator filled capillaries we used 3 mm diameter halar capillaries filled with an isopropyl biphenol base scintillator with a total hole packing fraction of 19%, core fraction 11%. The performance for this module was as follows:

$$\begin{aligned}\sigma/E &= 18.7\% \text{ for electrons @ 15 GeV} \\ 36 \text{ pe/GeV} &\text{ for 15 GeV electrons.}\end{aligned}$$

Figure 21 displays the pulse height distribution for the 15 GeV electron data, Figure 22 shows a scope trace of a sample signal.

For the quartz fiber tests the flexible capillaries were removed and a bundle of five 1 mm diameter quartz fibers inserted into each hole. The fibers used were 3M:TECS hard clad quartz fibers with a 1 mm core and 1.6 mm buffer diameter. The effective core packing fraction for this configuration was $\sim 7\%$. Data was taken with these modules longitudinal axis at an angle of 9° to the beam direction in the tests at BNL. Using 10 GeV electrons and muons we measured the following:

$$\begin{aligned}\sigma/E &= 25\% \text{ for 10 GeV electrons} \\ 3.5 \text{ pe/GeV} &\text{ for 10 GeV electrons}\end{aligned}$$

The phototube pulses from this quartz module are extremely fast with a rise time of a few nsec. The sample pulse is shown in Figure 23. Figure 24 displays the pulse height distribution for this quartz module in response to 10 GeV electrons and muons.

VI. R&D Program

In order to bring *any* of the potential FCAL technologies to the level needed for the final GEM design will require a substantial R&D effort in FY '93. This statement is meant to include even the liquid argon FCAL program. Further many of the points that require further study are shared by all these systems.

The main elements of the FY '93 R&D program needed for the scintillating liquid/cherenkov sampling calorimeters that we have described can be summarized as follows:

- Evaluate and test a suitable rad hard active medium.
- Simulate complete detector performance.
- Optimize the location of the FCAL for neutron leakage, E_T resolution and activation.
- Complete the final engineering design.
- Construct and test a > 10 T prototype using the final chosen technology.

It is worthwhile to point out that interest in this program is relatively broad within the GEM Collaboration. There is a strong overlap with the work being carried out by the SSCintCAL group on spaghetti calorimetry for the central and end wall regions in GEM, as well as with SDC's forward calorimeter group also working on a liquid scintillator approach to this problem. Once the choice of technology for the central hadron calorimeter is made we should have an adequate sized team to carryout this program successfully.

VII. Summary

We have presented here the design for a scintillating/cherenkov sampling spaghetti calorimeter for the forward region in GEM. This design integrates easily with the projective scintillating fiber hadron calorimeter option of GEM and provides the projective, hermetic, high performance hadron calorimetry needed in this program. This proposed FCAL has fast signal response time and is known to be rad hard to a level of 100 MRad or more. The technologies proposed here have all successfully been tested in prototype *em* calorimeters as described in the section on recent beam tests. These tests demonstrate that these devices should provide the performance required for a viable FCAL system at the SSC.

There are a number of issues that remain to be resolved through an active R&D program in FY '93 as outlined above. With the team that has been assembled, and with a reasonable R&D allocation for FY '93, we should be able to successfully deal with these questions and proceed to the final FCAL design.

References

1. JETSET Collaboration performance article.
2. SPACAL Collaborations paper on speed of spaghetti calorimetry.
3. R. Wigmans response to the Hybrid Group on Rad Hardness.
4. SSCintCAL's hadron calorimeter design for GEM.
5. TAMU/Fairfield Liquid capillary FCAL design.
6. Results received from J. White and colleagues on GEANT calculations for the SDC FCAL.
7. Results of irradiations of quartz disc by P. Gorodetzky.
8. Design work performed by Steve Chae, ORNL.
9. Discussion of shower shape analysis using BaF₂ calorimetry. One can find centers of showers to fractions of the tower size by doing energy weighted averages.
10. SPACAL shower shape measurements. NIM....
11. Results of P. Gorodetzky reported at RADAM '92.
12. Quartz Rad hardness references again.
13. Results of TAMU tests on radiation damage to mineral oil based scintillators.
14. Shower shape fitting and hadron calorimeter position resolution in the forward region in CDF. TAMU NIM
15. MC simulation work by Steve Dye, Boston University.
16. MC simulation work by Tarkovsky, ORNL.

Tables

- Table I. Table of various materials showing their level of radiation hardness.
- Table II. $\eta\phi$ boundaries for the *super towers*. in the spaghetti FCAL.
- Table III. Shower shape parameters from the SPACAL paper on shower shape.
- Table IV. Table of GEANT results showing the stochastic and constant terms for the SDC liquid scintillator geometry as a function of the capillary attenuation length. Courtesy of James White, TAMU.

TABLE I

GENERAL RELATIVE RADIATION EFFECTS CABLE INSULATION AND SHEATH MATERIALS

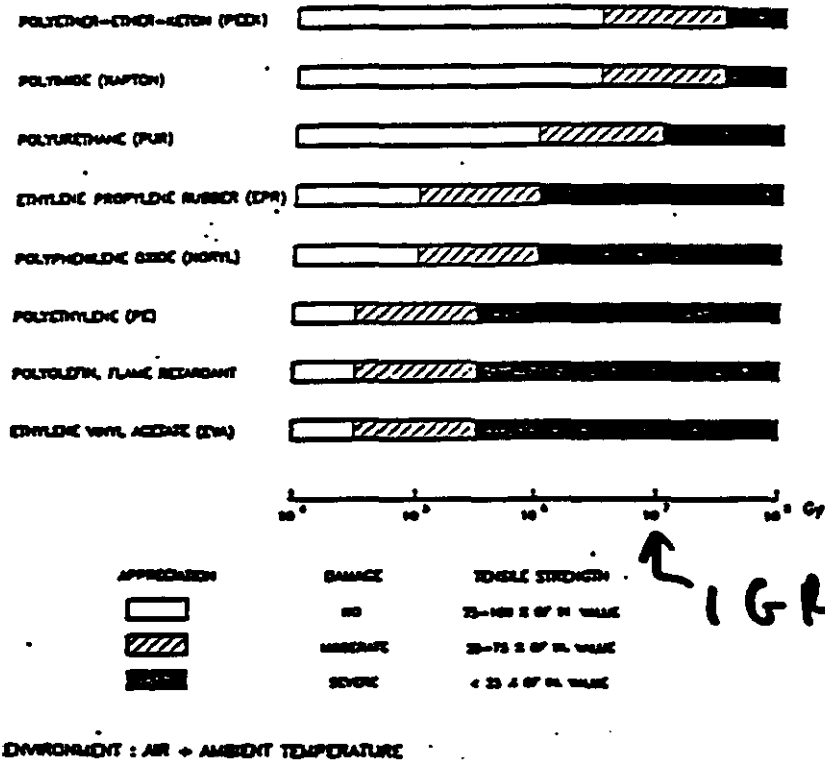


Figure 7: Radiation resistance of some polymers from a CERN report. Note the highest 3 will be investigated as claddings using commercial tubing manufacturers as the tubing sources.

E (GeV)	B_1 (pC/cm)	λ_1 (cm)	B_2 (pC/cm)	λ_2 (cm)
150	2.86 ± 0.06 (2.85)	14.3 ± 0.2 (14.4)	17.20 ± 0.38 (17.20)	3.63 ± 0.05 (3.64)
80	1.66 ± 0.04 (1.65)	14.3 ± 0.2 (14.5)	7.98 ± 0.18 (7.98)	3.80 ± 0.05 (3.81)
40	0.86 ± 0.02 (0.83)	14.3 ± 0.2 (14.7)	3.61 ± 0.09 (3.63)	3.91 ± 0.07 (3.94)
20	0.46 ± 0.01 (0.43)	14.6 ± 0.2 (15.5)	1.53 ± 0.04 (1.55)	3.95 ± 0.08 (4.03)
9.7	0.22 ± 0.01 (0.20)	14.1 ± 0.1 (16.0)	0.67 ± 0.02 (0.68)	4.08 ± 0.12 (4.22)
5	0.09 ± 0.01 (0.07)	13.5 ± 0.8 (17.7)	0.20 ± 0.02 (0.21)	7.71 ± 0.54 (7.68)
all	$(0.0209 \pm 0.0003)E$	14.1 ± 0.1	$(0.092 \pm 0.001)E$	3.83 ± 0.04

TABLE III

TABLE I

1 Meter Diam. Det; 3 Meter length; Fe Absorber.

Particle enters @ 3° , Center to Center distance

@ twice of hole diam.

Hemisphere length :		2m	3m	4m	5m	∞
Hole Diam 2mm (4mm ϕ to ϕ)	A(%)	10	5.8	4.7	4.6	1.3
	B(%)	78	70	66	60	55
3mm (6mm ϕ to ϕ)	A(%)	15*	10*	9.4*	7.5*	3.7*
	B(%)	40	30	46	51	54
5mm (10mm ϕ to ϕ)	A(%)	14	11	9.4	7.7	6.4
	B(%)	-	37	45	58	53

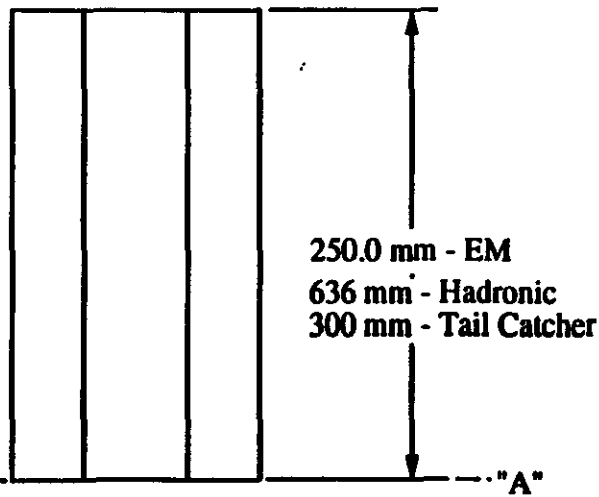
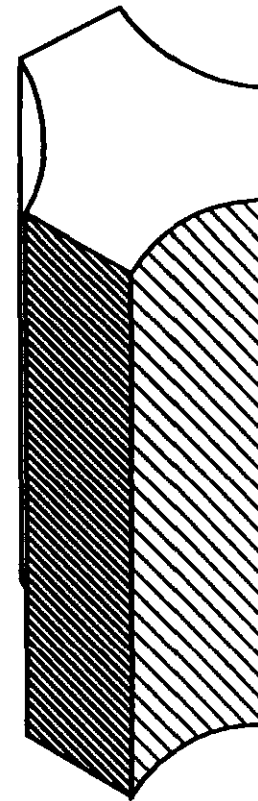
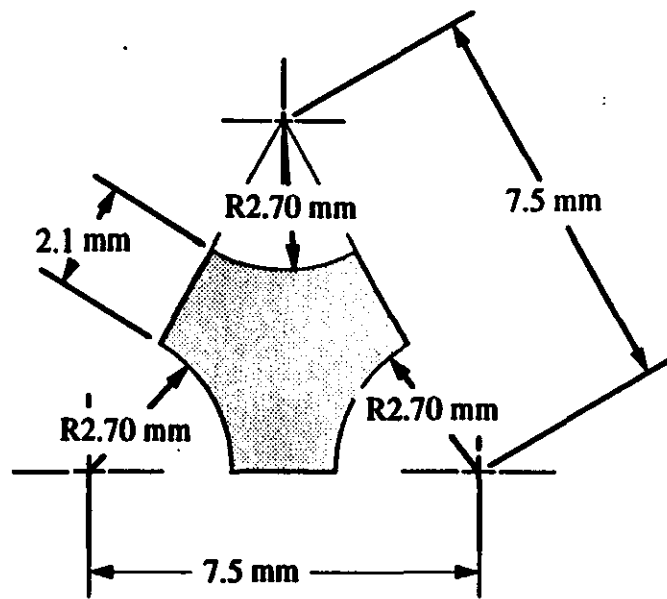
* NOT GOOD FITS

Figure Captions

1. Design of the tungsten pellet for the forward calorimeter.
2. Hole pattern produced by stacking these tungsten pellets.
- 3a. FCAL assembly.
- 3b. HYBRID Calorimeter assembly showing the fiber FCAL.
4. $\eta\phi$ boundaries for the FCAL *supertowers*..
5. Results of MC studies by P. Gorodetzky on the amount of cherenkov light emitted by a single fiber for $\beta = 1$ particles as a function of impact parameter and angle to the axis of the fiber.
6. Results of a similar MC calculation performed by Tarkovsky at ORNL.
7. SPACAL Collaborations lateral shower profile.
- 8a. Radiation damage effects for a quartz wafer as a function of radiation dose and light wavelength. Gorodetzky
- 8b. Radiation damage measurements of a quartz fiber. Gorodetzky
- 8c. Radiation damage of a 1" diameter, 1" long piece of pure quartz as measured by TAMU and BNL groups for GEM.
- 9a. Radiation hardness of toluene based scintillating liquids.
- 9b. Radiation damage of a Bicron liquid formulation.
10. Light attenuation length measurements for a 2 mm diameter stainless steel capillary using a PDMS coating.
11. Optical transmission of quartz as measured by Heraus.
12. Light attenuation measurements for a 2 mm diameter unclad quartz rod.
13. MC resolution for a quartz fiber calorimeter.
14. Hole pattern in the TAMU em prototype calorimeter.
15. Assembly of a single TAMU em module.
16. Schematic of a 7 tower stack of em modules.
17. Response of the TAMU stack to cosmic ray muons.

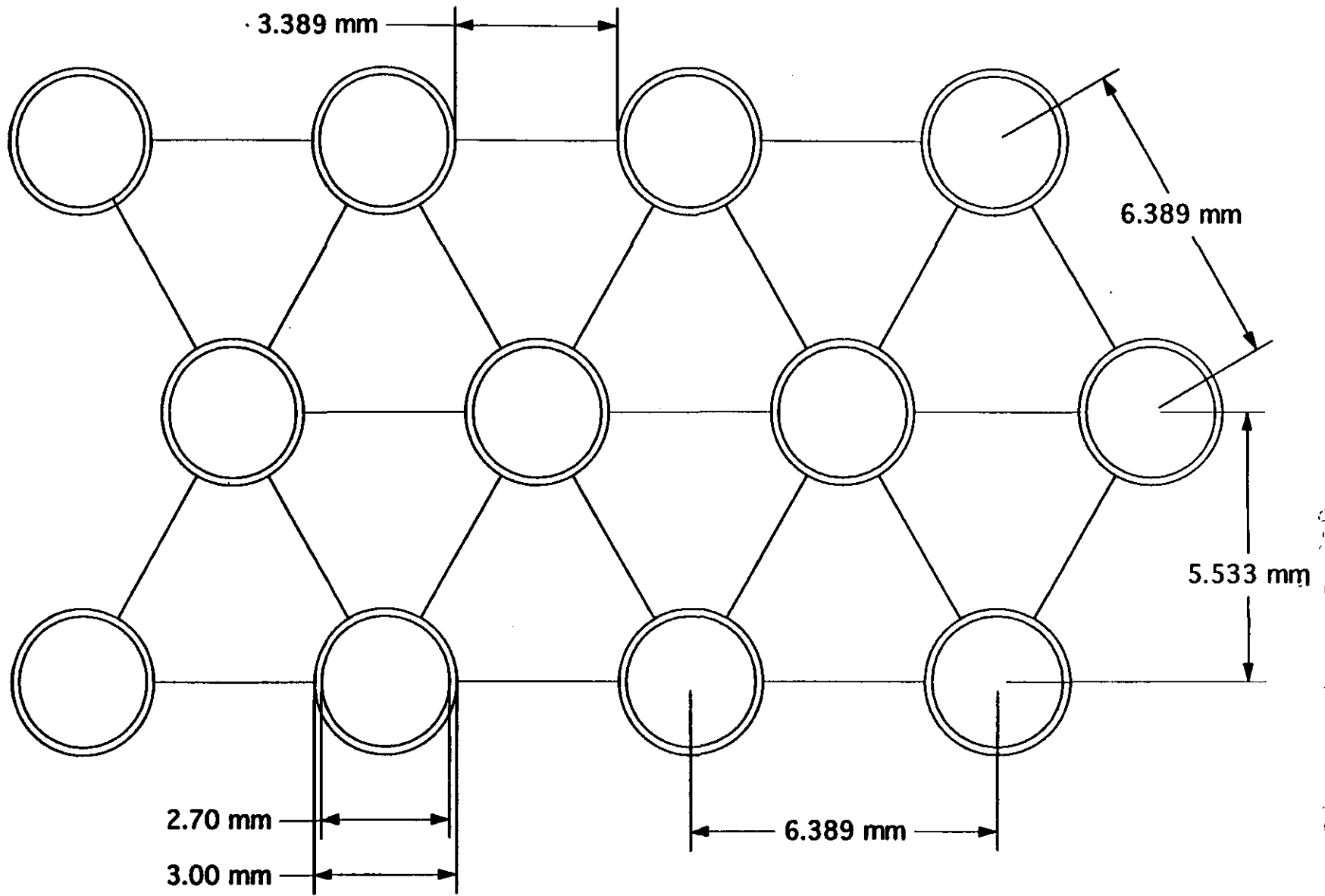
18. Typical ADC distribution from one of the 7 modules tested at BNL.
19. Summed pulse height distribution for 10 GeV electrons at BNL. Also displayed on this plot are the fitted values for a gaussian.
- 20a. Fairfield prototype hole pattern.
- 20b. Fairfield prototype lead stack with phototube.
21. Response of the Fairfield liquid filled capillaries to a 15 GeV electron beam.
22. Storage scope trace of the phototube pulse from the liquid filled module.
23. Storage scope trace of the phototube pulse from the quartz fiber module.
24. Response of the quartz fiber calorimeter module to 10 GeV electrons.

Figure 1
Dollot
LAR
Design



Module 1	Module 2	Module 3
2.70 mm	2.93 mm	3.18 mm
2.10 mm	2.34 mm	2.59 mm
7.50 mm	8.20 mm	8.95 mm

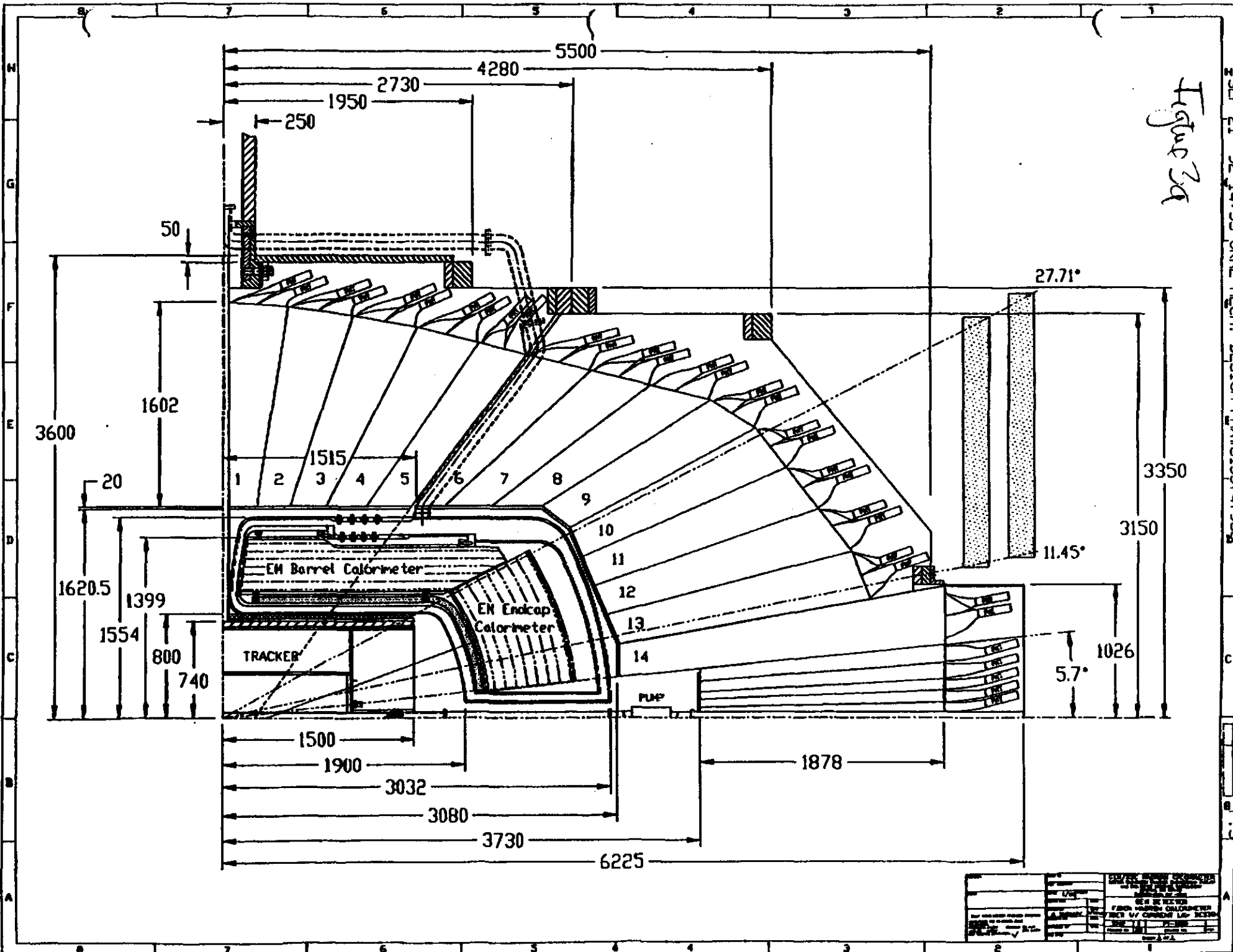
FCAL MODULE - DEFORMED TUNGSTEN FILLER DETAIL



*Figure 2a
side section ICH*

SPAGHETTI TUNGSTEN PELLETS & TUBE ARRANGEMENT

Figure 2a



DATE	10/1/92	DESIGNED BY	W. J. BROWN
APP'D		CHECKED BY	W. J. BROWN
REV		DATE	
PART NAME		EM END CAP CALORIMETER	
PROJECT		EM END CAP CALORIMETER	
DRAWN BY		W. J. BROWN	
SCALE		AS SHOWN	

DATE	12/11/92
BY	J. J. ...
CHECKED BY	...
DESIGNED BY	...
SCALE	AS SHOWN
PROJECT NO.	...
DRAWING NO.	...
REVISIONS	...

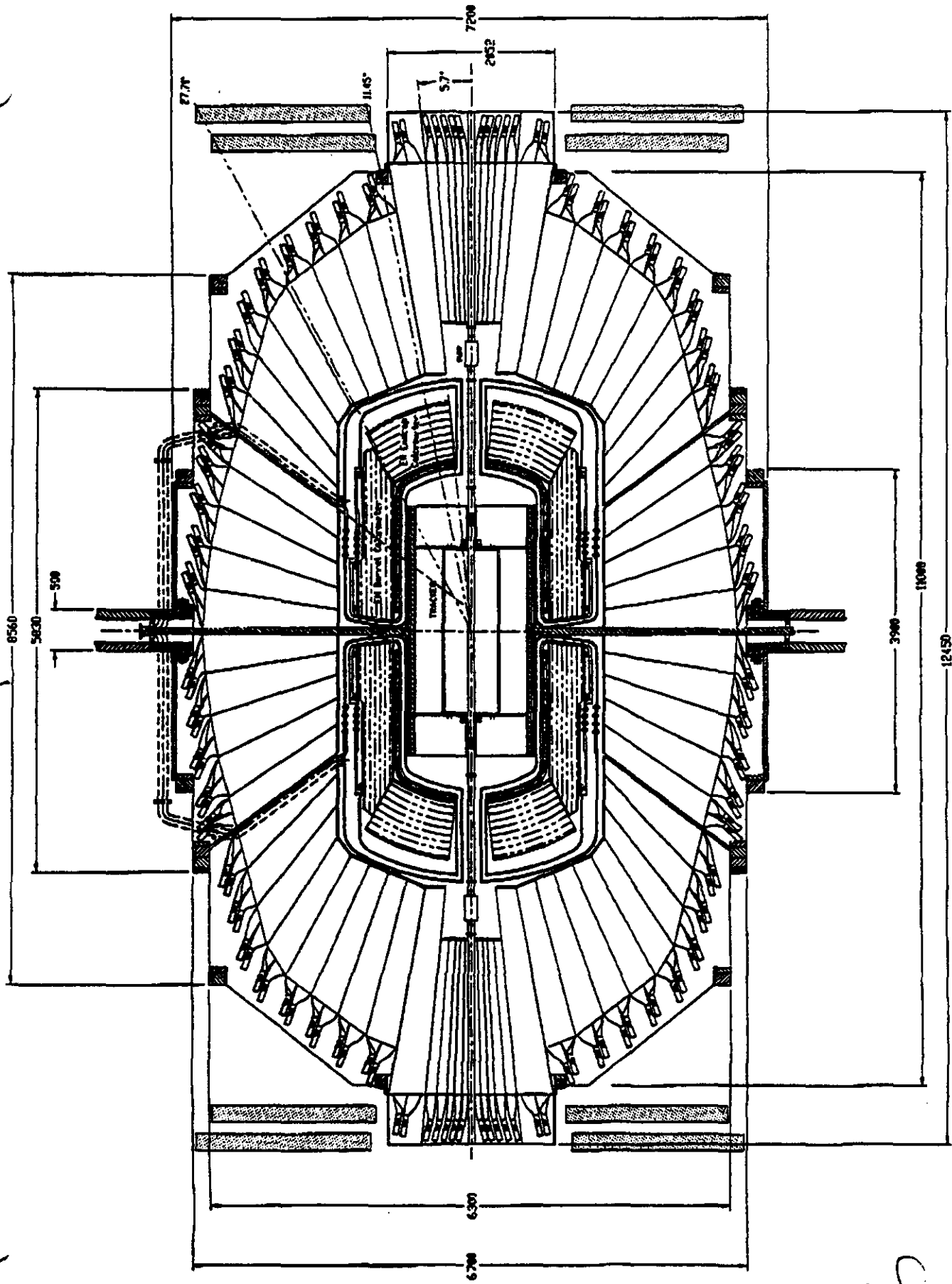
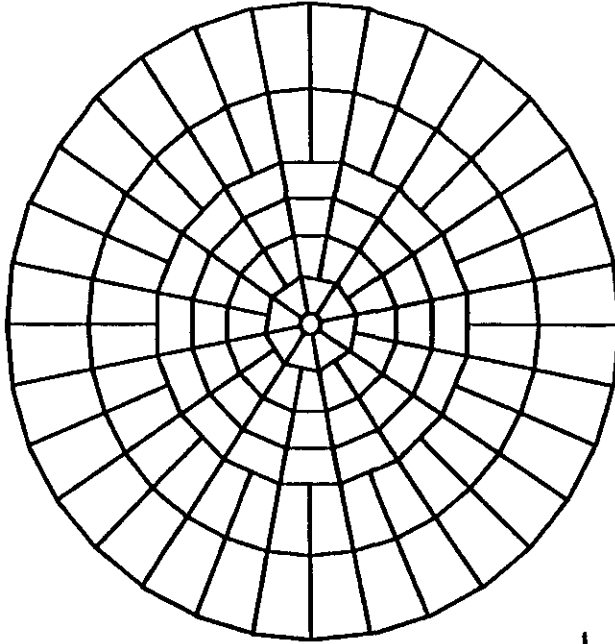
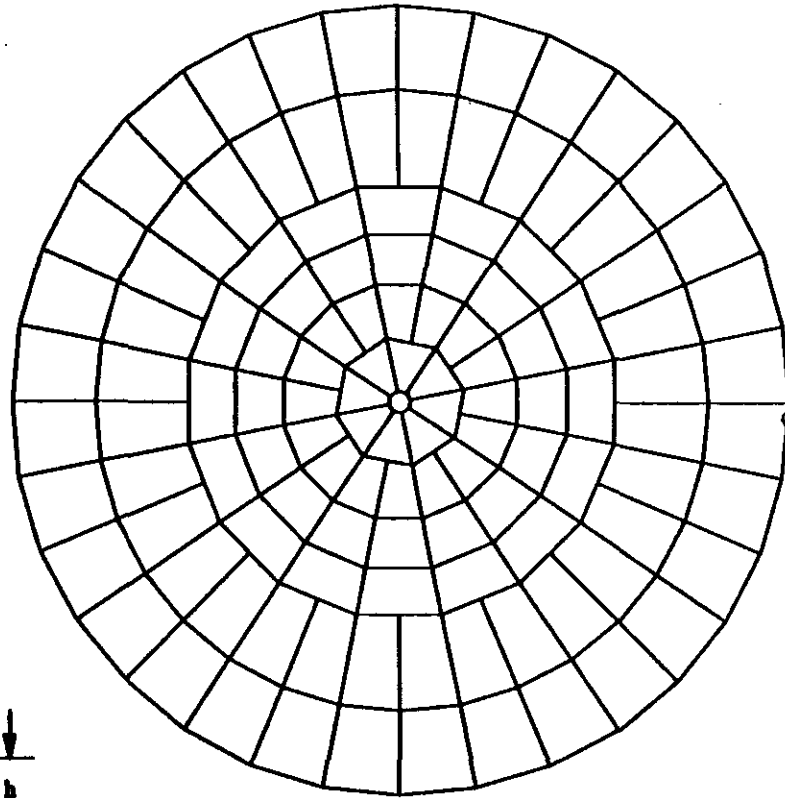


Figure 36



INNER FACE
 @ 4720 mm FROM IP



OUTER FACE
 @ 6582 mm FROM IP

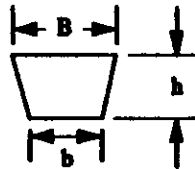
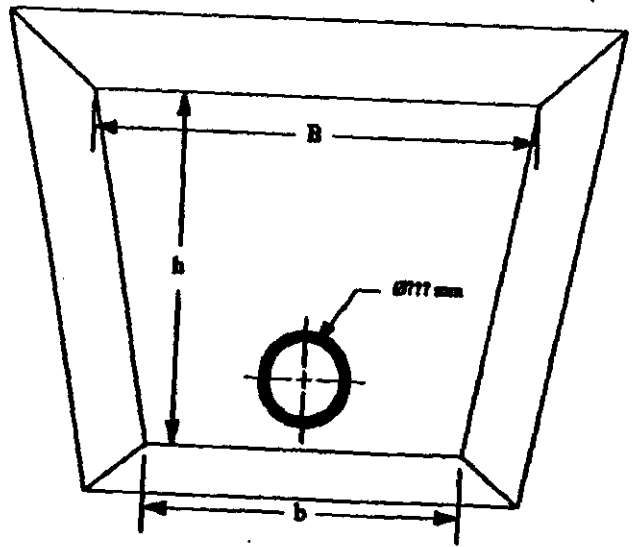
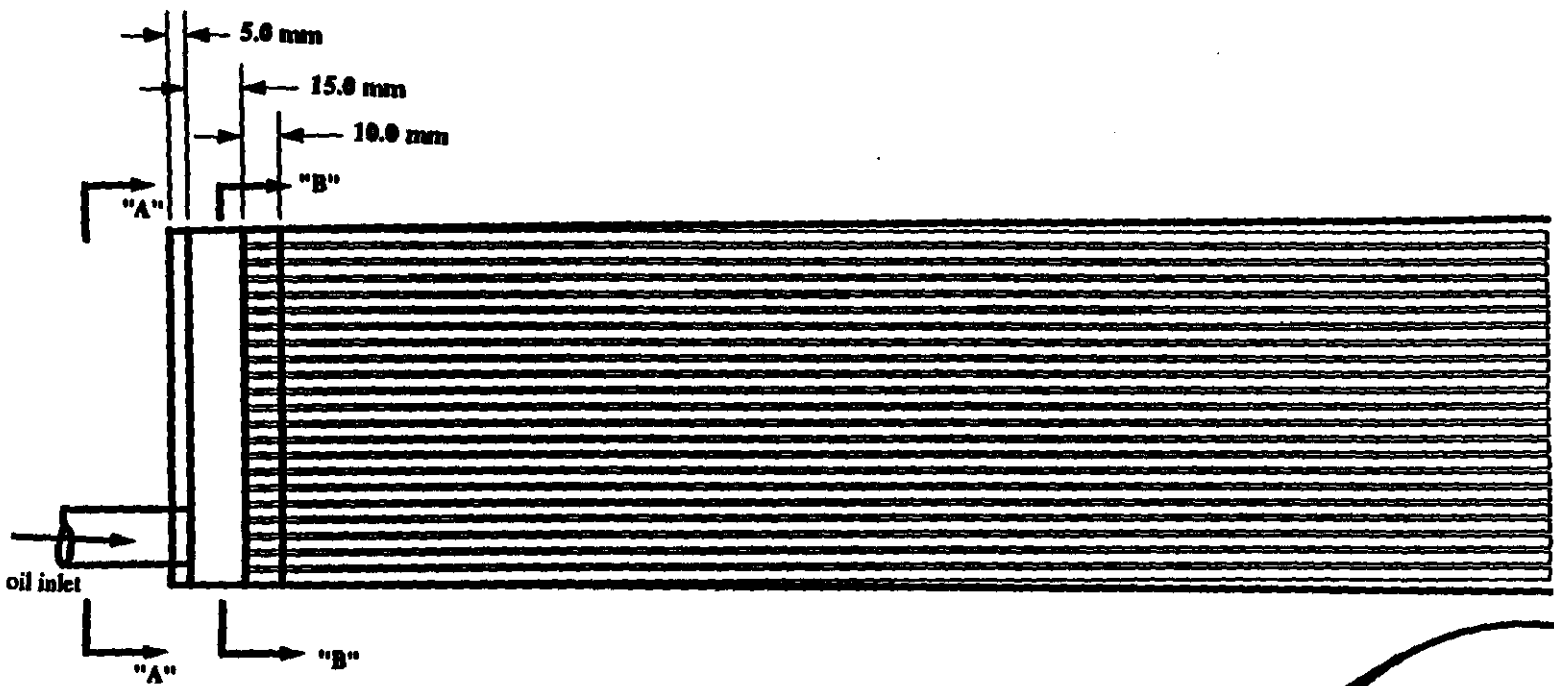


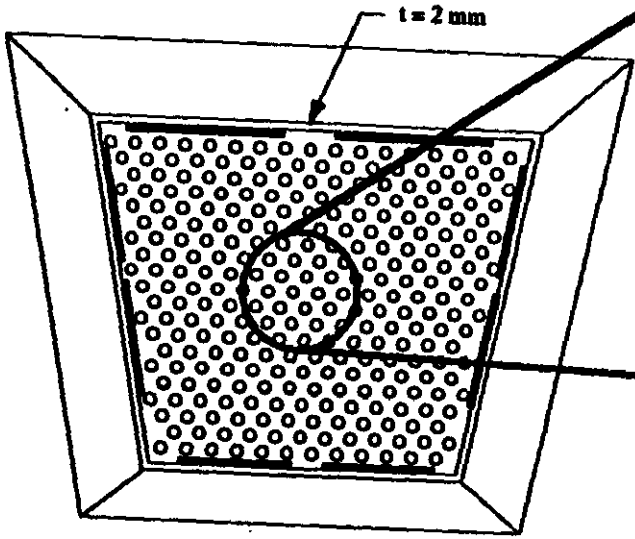
Fig 4a
of layout for particle design
of FCL.

Module Number	@ 4720 mm from IP		@ 6582 mm from IP		@ 4720 mm from IP			@ 6582 mm from IP		
	Eta	Radius mm	Eta	Radius mm	B mm	h mm	b mm	B mm	h mm	b mm
6	6.378	25.00	6.378	25.00	77.85	69.07	19.13	108.57	105.42	19.13
5	4.550	99.77	4.550	139.13	70.95	80.45	38.93	98.93	112.17	54.28
4	3.950	181.83	3.950	253.55	100.72	74.75	70.95	140.47	104.19	98.93
3	3.600	258.13	3.600	360.02	130.01	71.96	100.72	181.32	100.27	140.47
2	3.350	331.60	3.350	462.32	92.36	138.38	65.01	128.80	192.75	90.66
1	3.000	471.16	3.000	657.03	131.57	199.01	92.36	168.01	199.01	128.80
OD	2.649	671.16	2.740	857.03						

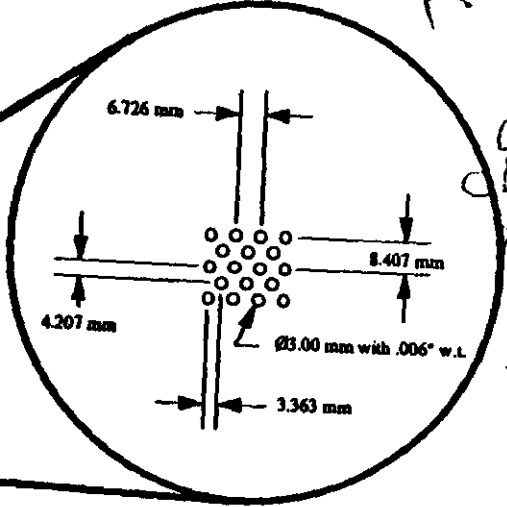
MARTIN MARIETTA ENERGY SYSTEMS	
PROJECT: SSC GEM DETECTOR	
FORWARD CALORIMETER LIQUID SCINTILLATING OPTION SPAGHETTI TOWER & MODULE DESIGN	
PRINT NO: D-FCLS-TAMD001	REV 6
DRAWN BY: S. M. CHAI	3/31/92
CHECKED & APPROVED BY:	



VIEW "A-A"



VIEW "B-B"



TUBE ARRANGEMENT DETAIL

MARTIN MARIETTA ENERGY SYSTEMS	
PROJECT: SSC GEM DETECTOR	
FORWARD CALORIMETER LIQUID SCINTILLATING OPTION SUPER TOWER INNER END FACE DETAIL	
PRINT NO: D-FCLS-TAMD004	REV 1
DRAWN BY: S. M. CHAE	3/3/92
CHECKED & APPROVED BY:	

Note: 1. See DFCLSTAMD001 for dimensions B, b, and h.

Project Tower design
FCAL
Figure 4b

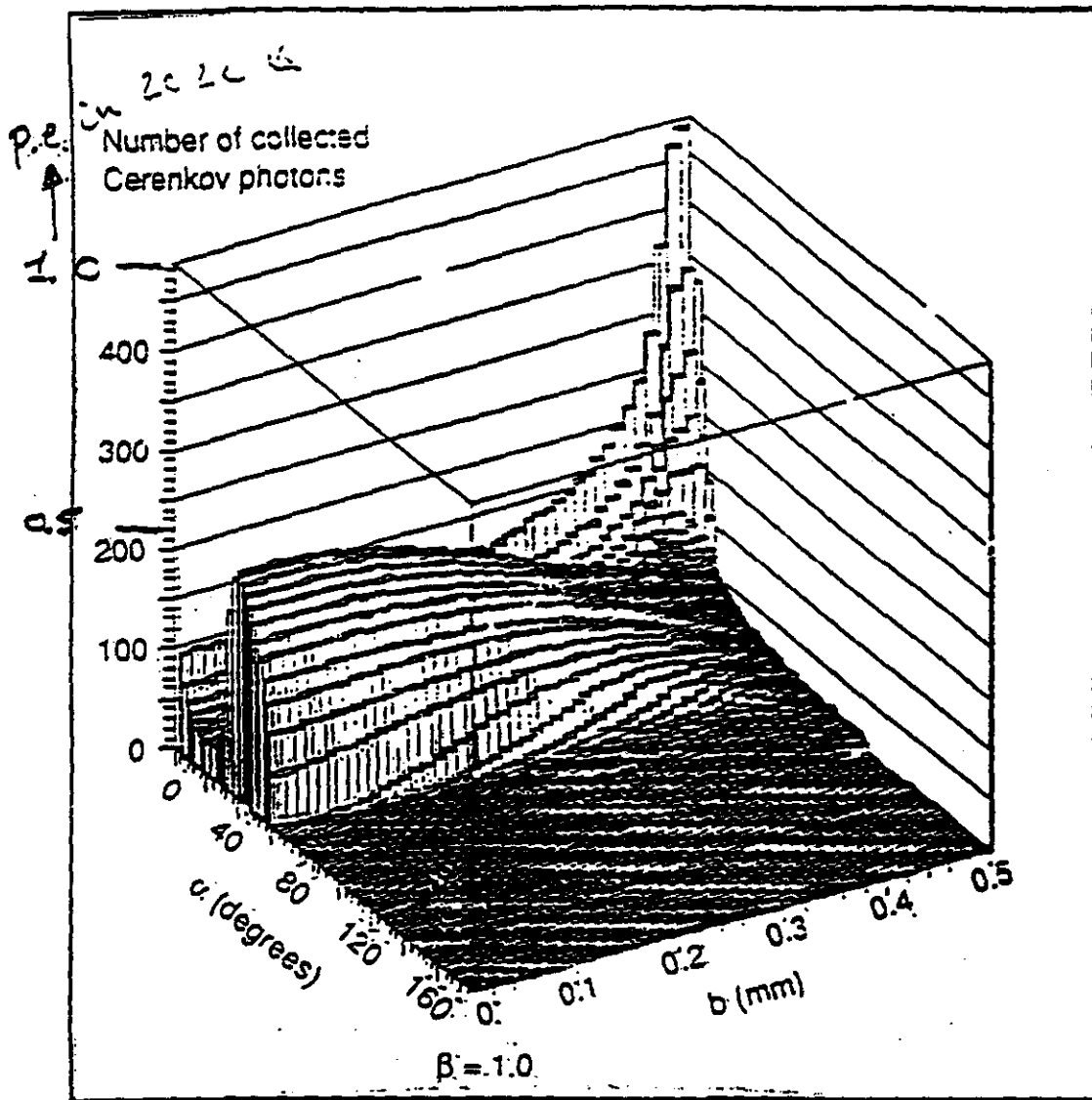
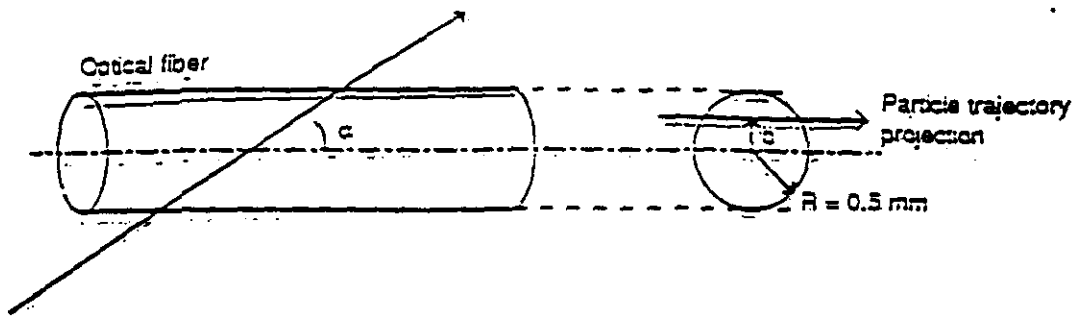
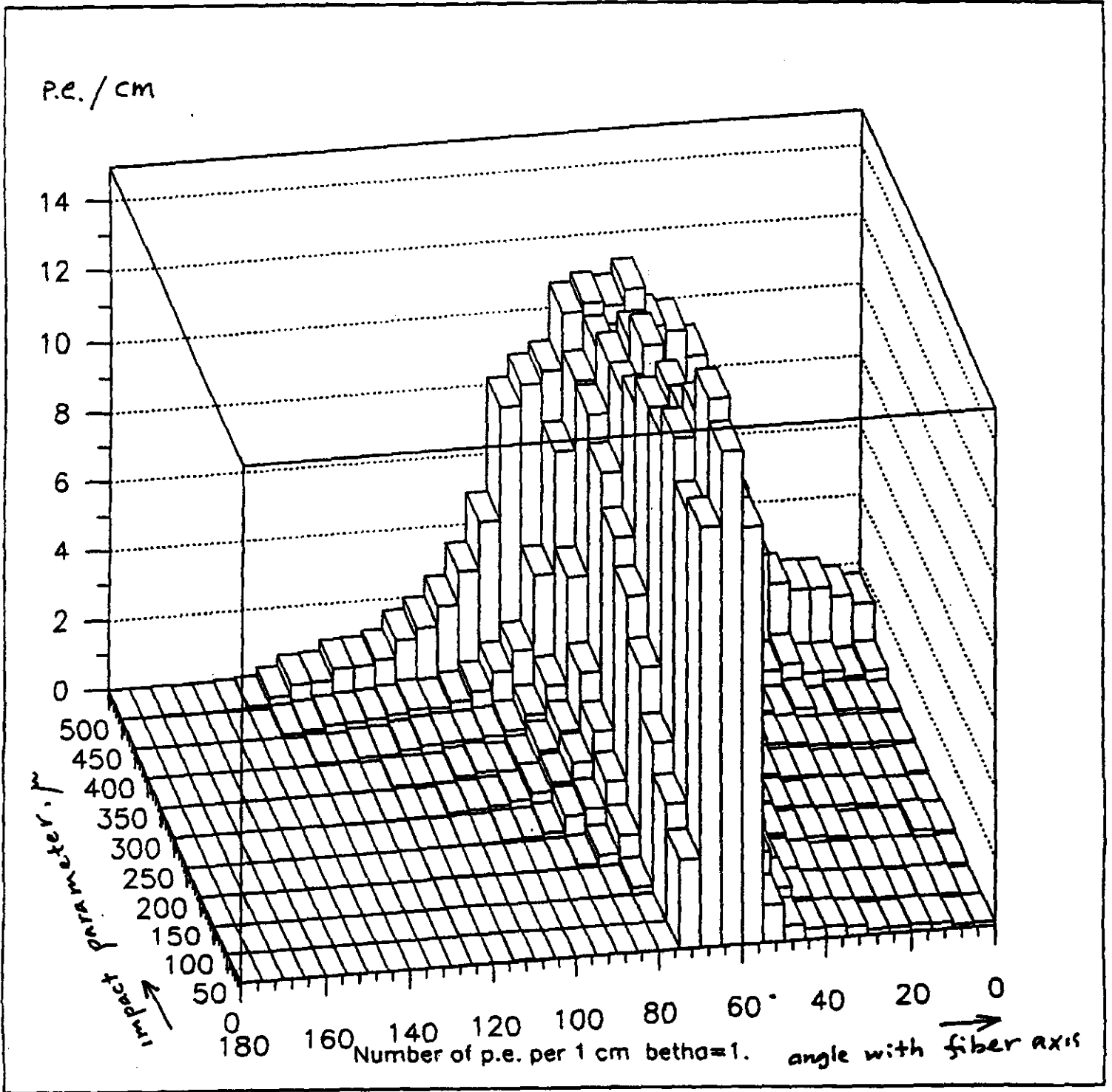


Figure 2 : Top) Geometrical parameters of an optical fiber - particle trajectory system. Bottom) Number of photons produced by Čerenkov effect and collected at the extremity of a fiber (1 mm diameter and numerical aperture of 0.37) intercepted by a charged particle ($Z=1, \beta=1$).

$\beta=1, \theta=0$ at $z=0$ through the center
of a fiber 1 mm thick gives 0.44 p.e.

Figure 5 - from A. Gorodetzky

quartz fiber ϕ 1mm
 core 1.53, cladding 1.51 @ 220nm



E. Tankovsky, ORNL
 Sept 21, 92

Figure 6a
 $\beta=1$

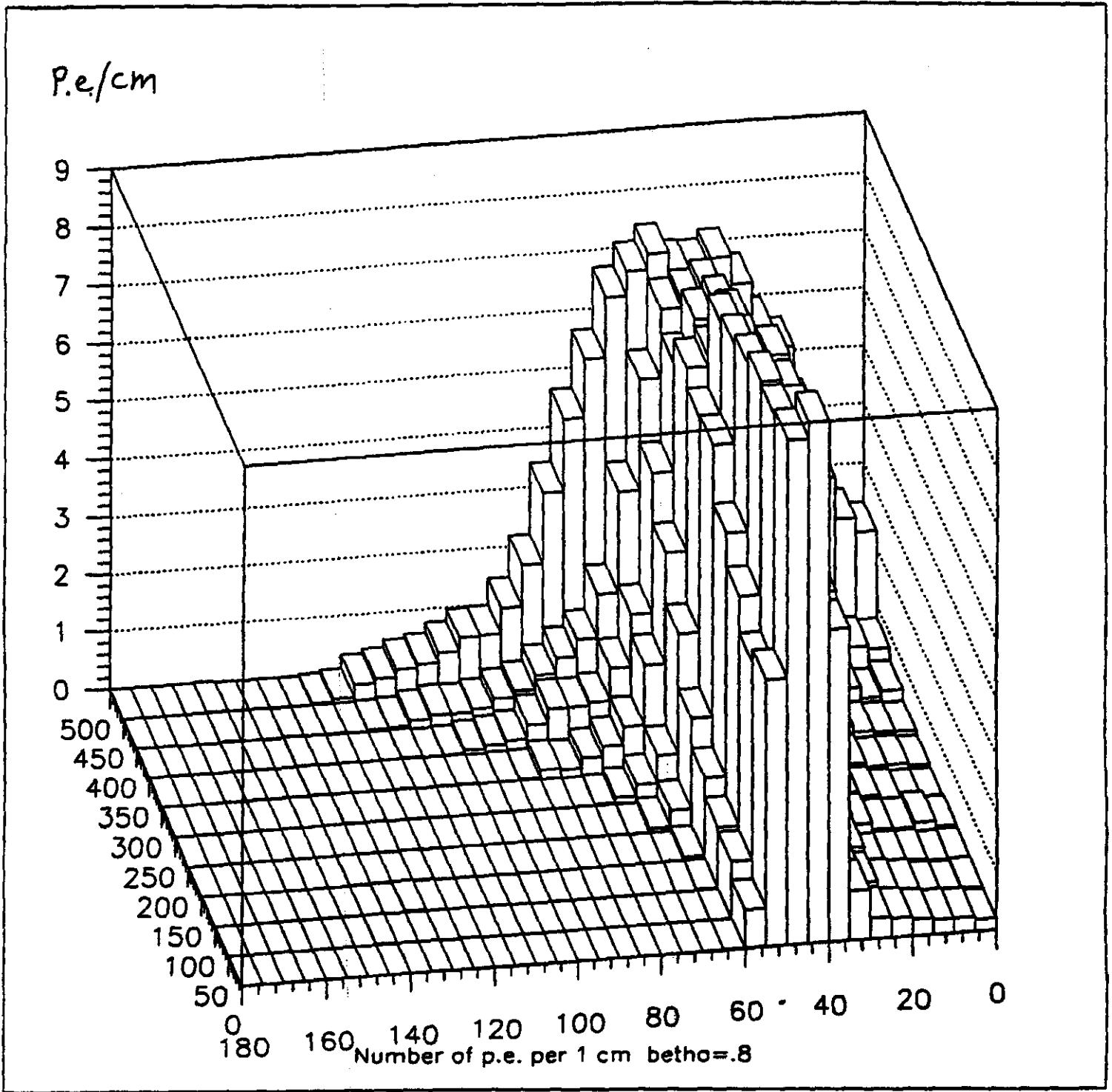


Figure 6b
 $\beta = 0.8$

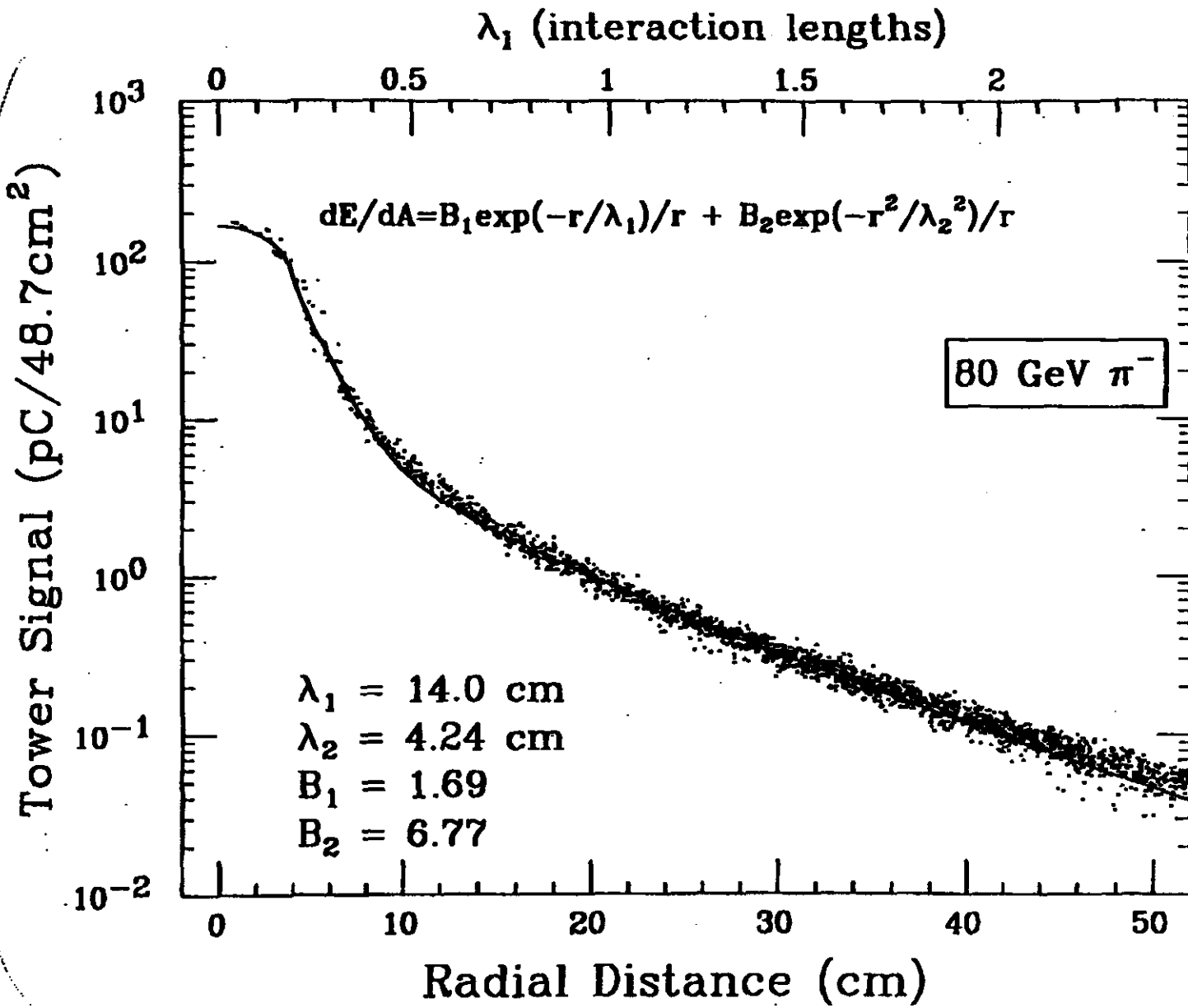
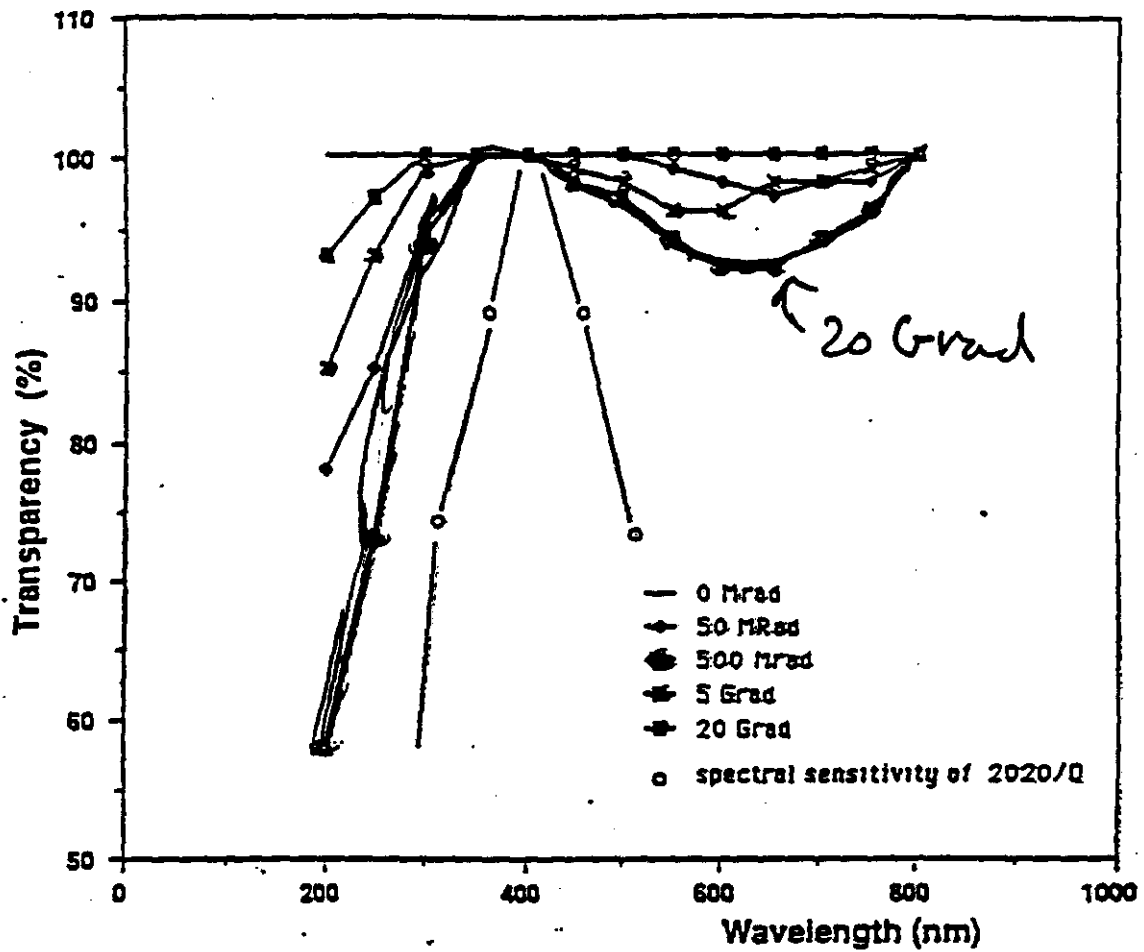


Figure 7
Transverse Shower Shape
SPMCH

Figure 8a

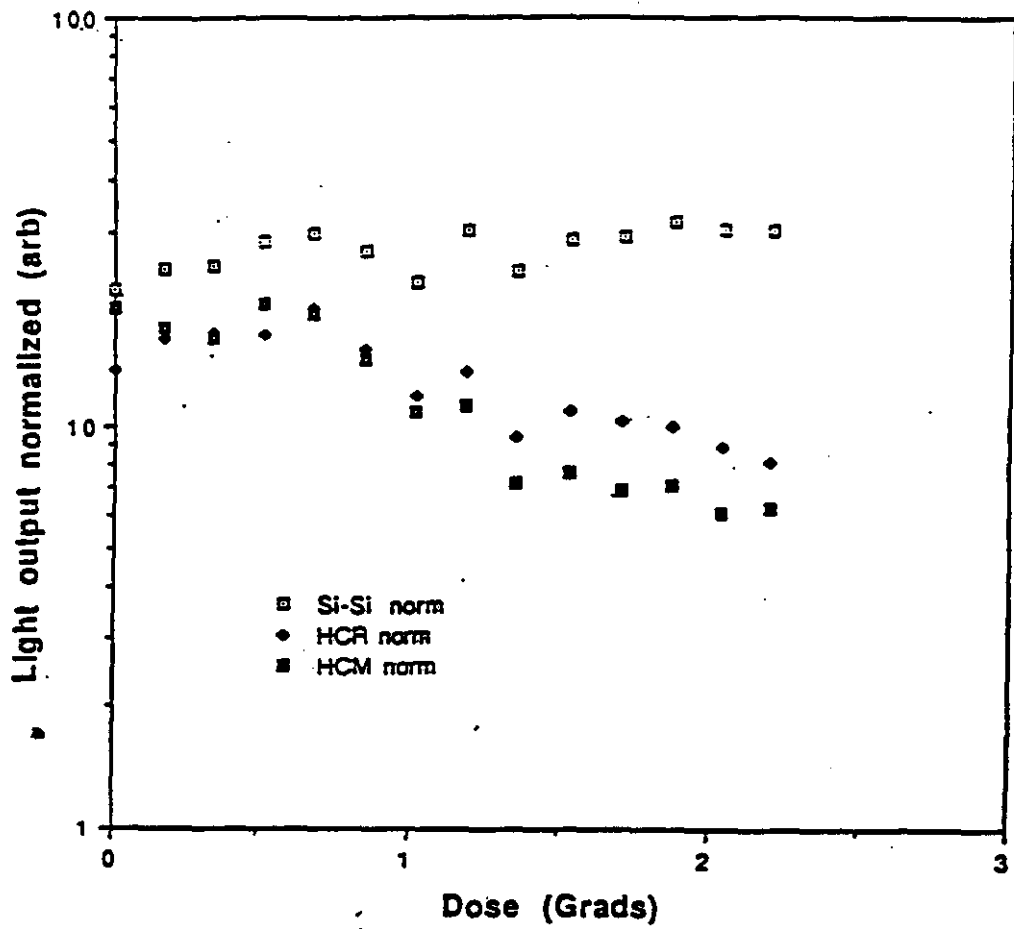


[Graded at 20 Grad]

Transparency of a 2 mm thick Suprasil quartz disc after different doses of irradiation. The spectral sensitivity of the 2020 Q photomultiplier shows the interesting fact that this wavelength range is the most insensitive to radiation.

Figure 3b

Quartz fiber irradiation with electrons



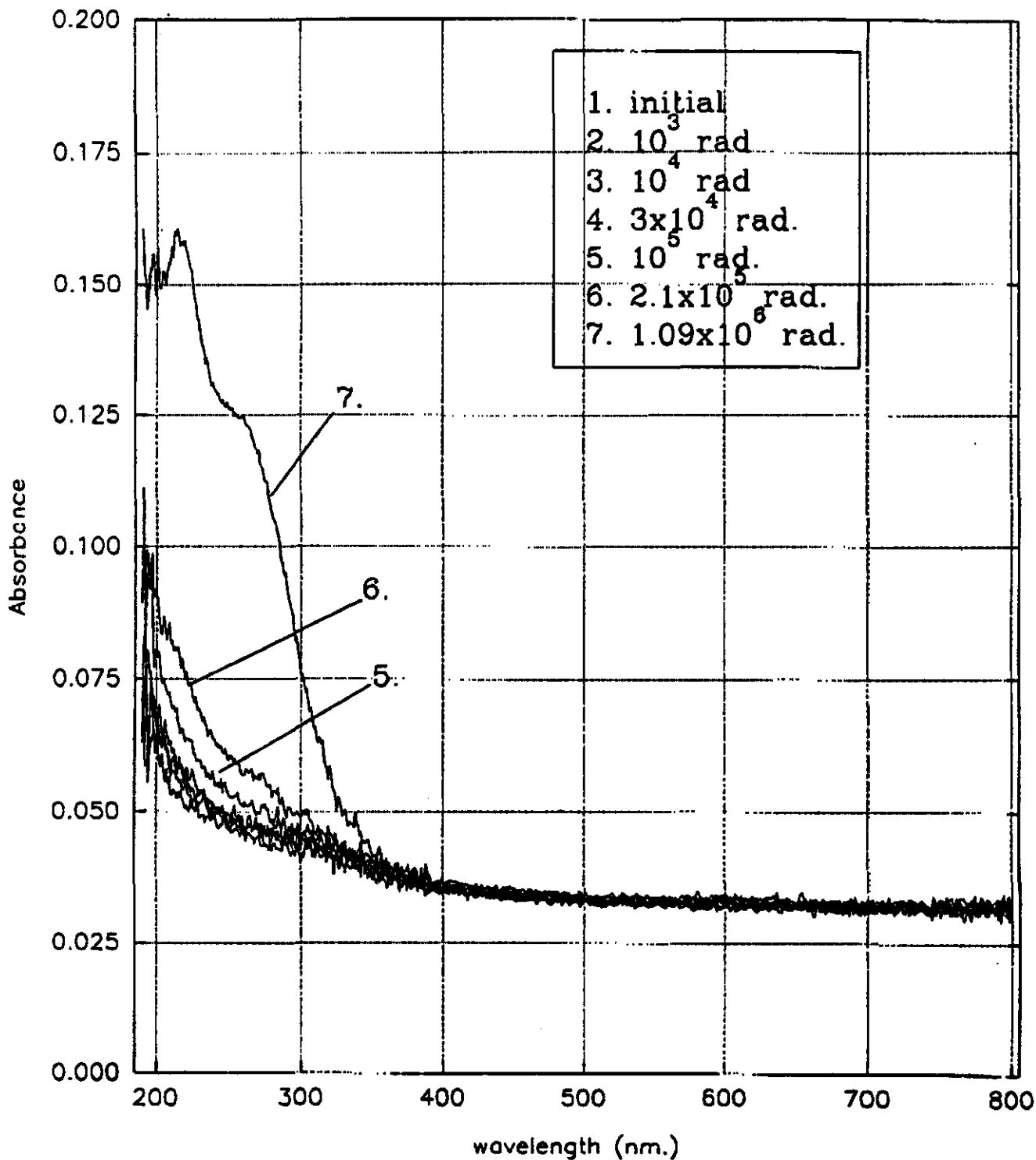
[Gondet et al.]

Figure 8c

Results of irradiation of quartz block
at BNL for ϕ_{Fe}

Quartz "B" (25mm x 27mm diam.)

9/23/92



Sean Stoll

Craig Woody
FRONT PHYSICS

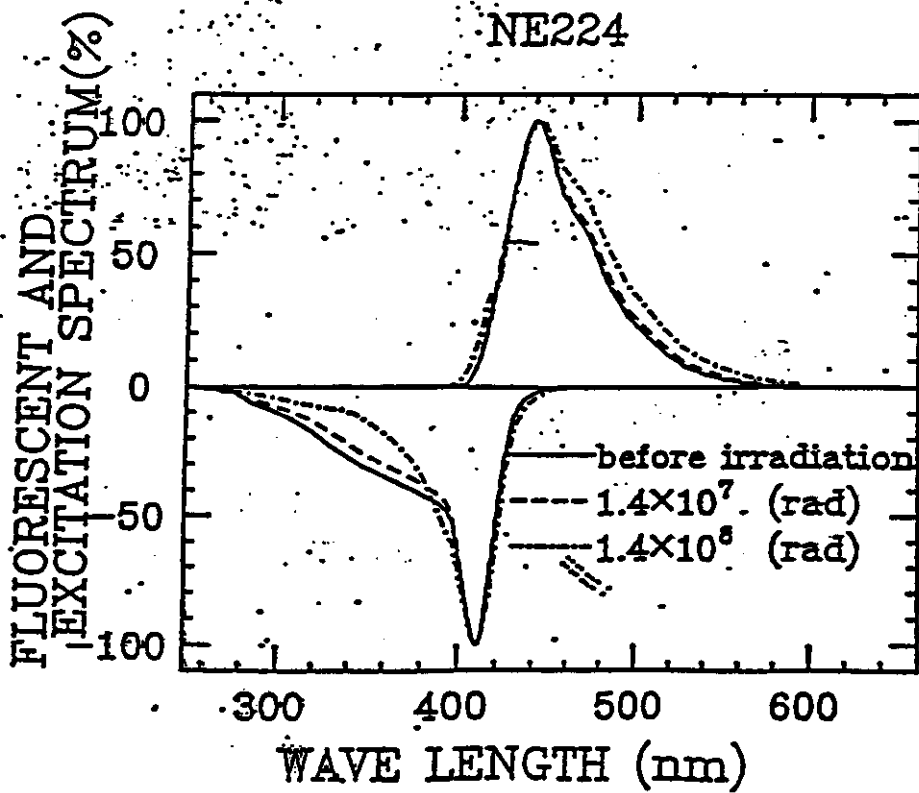
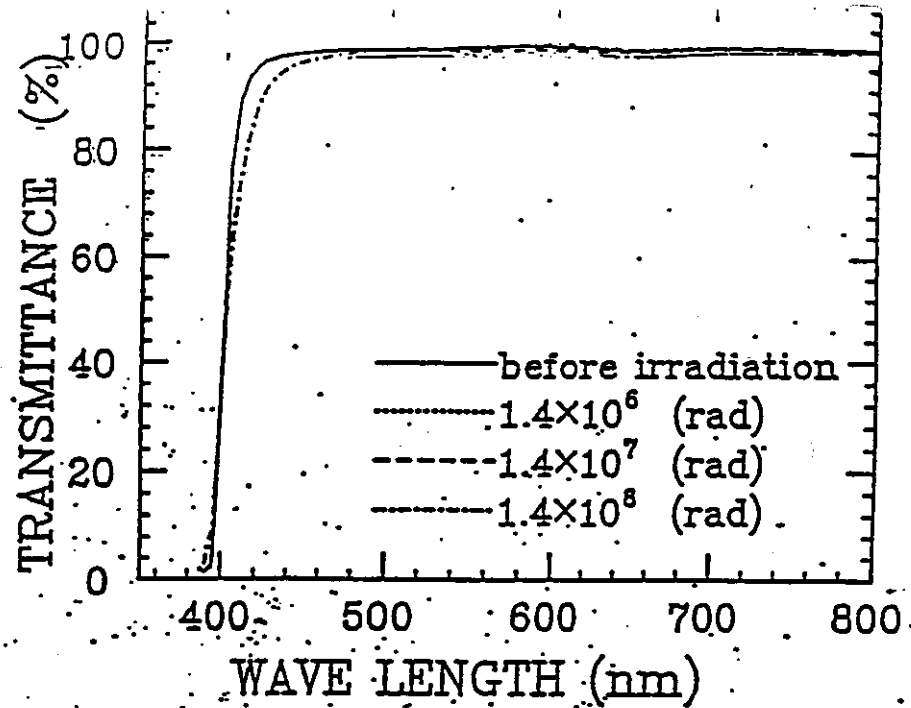
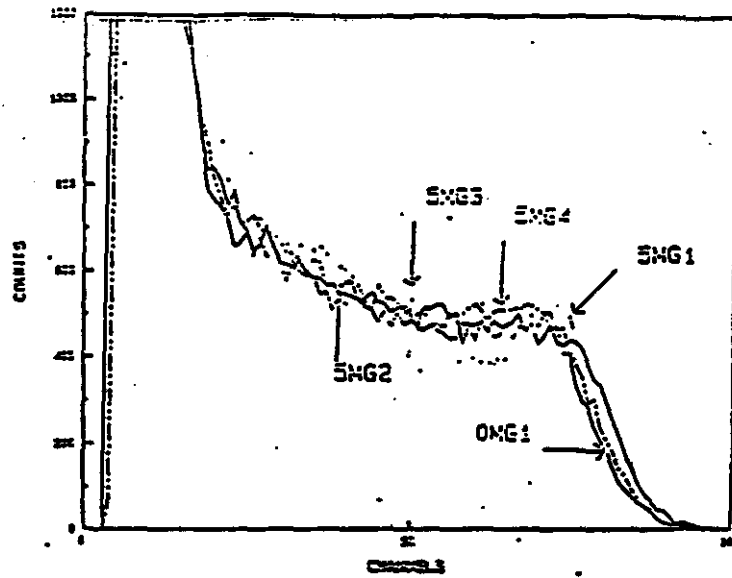


Figure 1: Typical toluene based liquid scintillator's (NE224) properties before and after 140 MRad [Chiba et al p 381, CDF Conference at Tsukuba, April, 1990, KEK publ.]

F2 SCINTILLATION



F2 TRANSMISSION

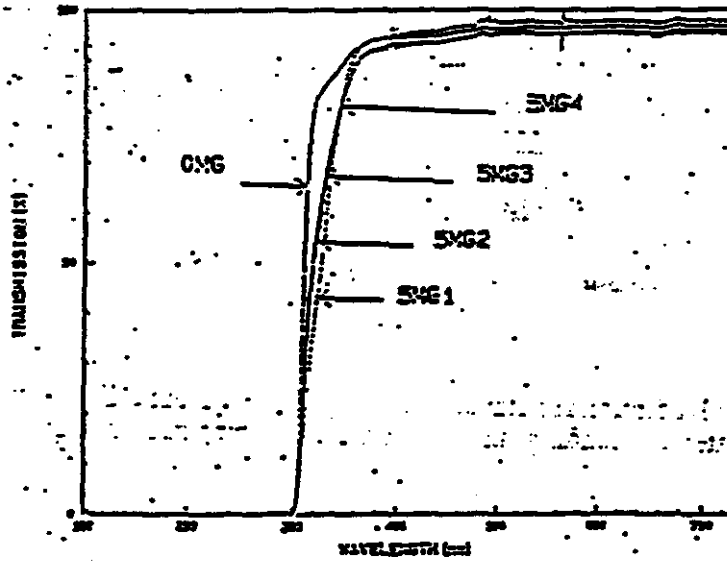


Figure 2: Bicron formulation after large doses of radiation [S. Majewski, CEBAF, private communication].

Figure 9b

MINUIT χ^2 Fit to Histogram 10

File: [ZAMAN.GRAPH]RESTEK3_NF_L8.GRAPH;2 21-JUL-92 17:20:44
 Areas: Hist 1438.22 Func Total/Fit 1437.97 / 1437.97

$\chi^2 = 0.9$ for 9 - 2 d.o.f., C.L. = 99.6%

Errors	Parabolic	Minos	
Function 1: COMIS Function XMNCMI			
A	176.50 ± 0.6377	+1.360	-1.350
B	299.00 ± 14.28	+23.30	-20.28

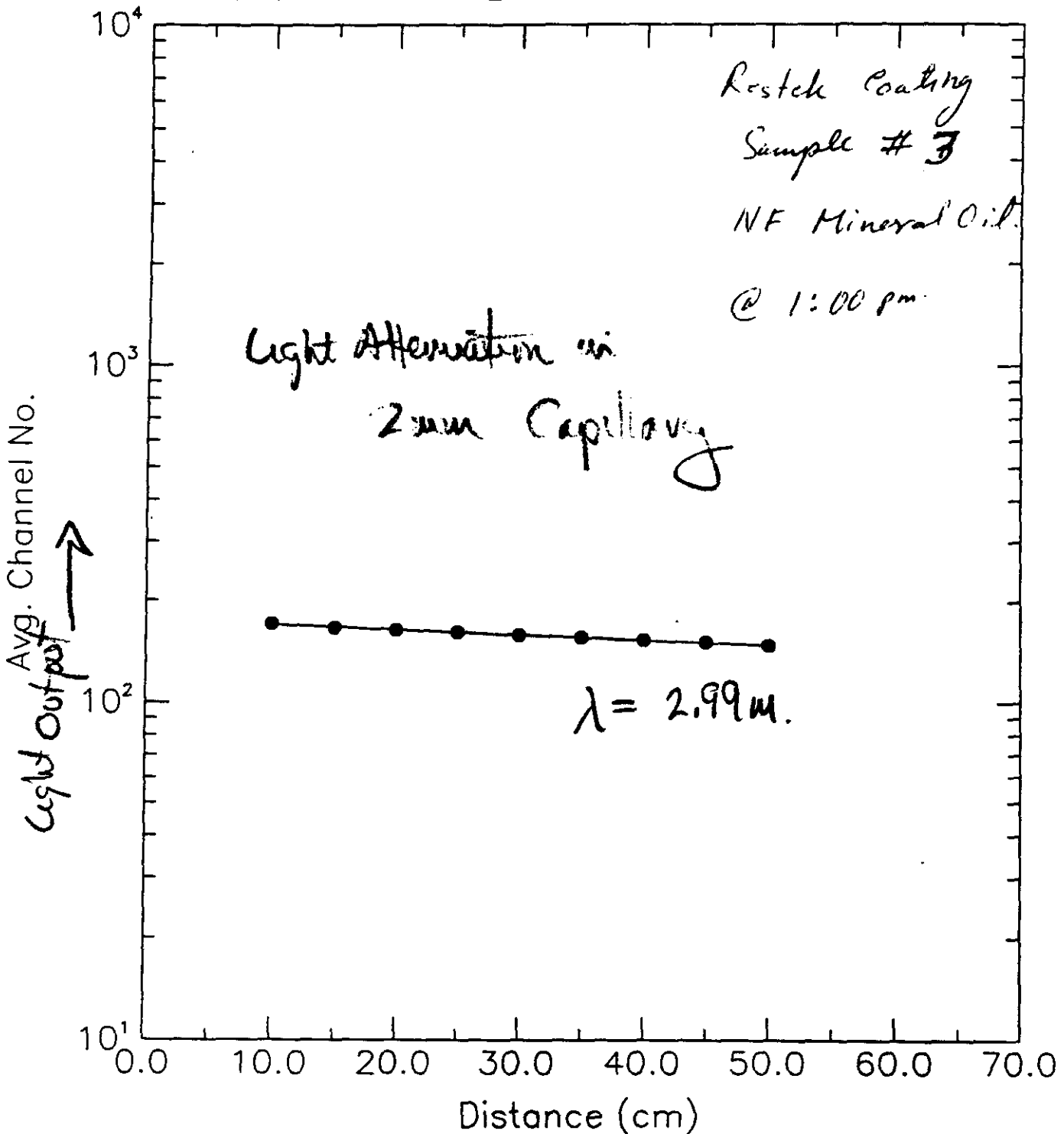


Figure 10

Optical Homogeneity—Suprasil and Suprasil-W are free from granular structure, are striae Grade A per MIL-G-174, and have a minimum index variation for application in the most precise instrumentation and optical system design. The Abbé Constant or dispersion factor for Suprasil would qualify under MIL-G-174 as Type 458-677. All synthetic fused silica material is slightly different in its Abbé Constant compared to that manufactured from crystalline quartz which is type 458-676. It should be noted, however, that the MIL tolerance (for type) is plus or minus 5. The refractive index of Suprasil-W more closely approximates the index of fused quartz made from natural crystal rather than other synthetic fused silica grades.

The number 2 grades of Suprasil and Suprasil-W have good index variation in one direction (perpendicular to the plane surfaces), as do the number 1 qualities. However, the number 1 qualities of Suprasil and Suprasil-W have a distinct advantage for prism applications, in that the low index variation can be maintained in all three directions upon special manufacture, making Suprasil 1 and Suprasil-W1 available as practically isotropic. The specification chart lists the maximum index variation. Suprasil and Suprasil-W are also available (on special order) to a higher isotropic homogeneity, such as that used in the Apollo retro-reflectors, of less than $1 \times 10^{-6}/\text{cm}$.

Suprasil and Suprasil-W both have exceptionally low bubble content. For discs and plates up to 10" diameter we guarantee the number 1 Types to be completely free of bubbles. (See note 5 on specification chart, pages 12 and 13.)

Purity—Suprasil and Suprasil-W grades, as with most synthetic materials, have extremely high purity. The metallic impurities in a typical analysis total approximately 1 ppm.

OH Content—The basic difference between Suprasil and Suprasil-W is the OH content, it being approximately 1200 ppm and 5 ppm respectively.

Fluorescence—All Suprasil grades are practically free of fluorescence. This characteristic and extreme purity makes Suprasil tubing most suitable for electron spin resonance and proton resonance spectroscopy.

Radiation Resistance—Against UV, gamma, X ray and other radiation, Suprasil and Suprasil-W are most resistant to discoloration. After electron radiations of one MeV and doses of 10^{15} e/cm², there is no discoloration, and only a very weak absorption band at 260 nm has been found with Suprasil-W.

Workability—Suprasil and Suprasil-W have excellent workability both for mechanical and flame re-working. The transmission properties for each of the grades are stable when re-working for lamp envelopes, test tubes and apparatus. Due to the exacting annealing cycle of the Suprasil grades, we do not recommend thermal removal of cutting and grinding strains. These stresses can normally be removed by careful edging or etching with hydrofluoric acid.

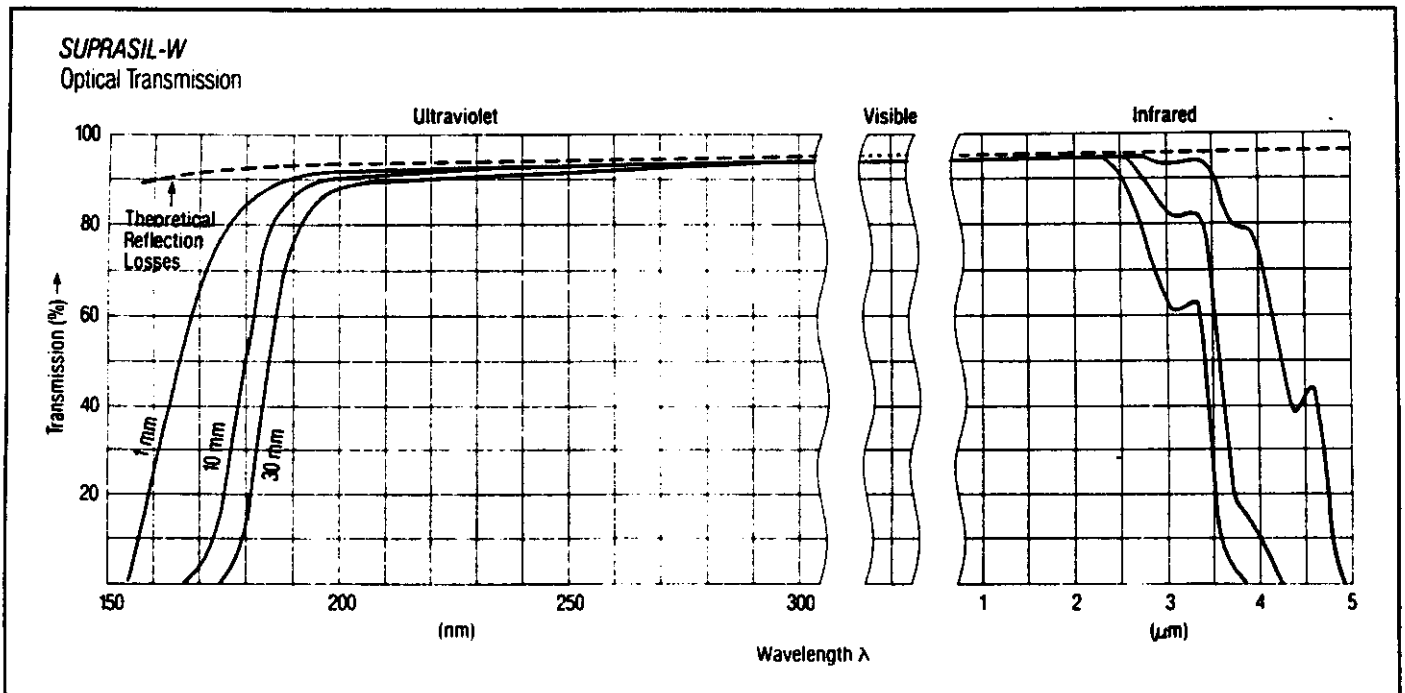


FIG. 3

Figure 11

File: Generated internally
 ID 98765 1 98765 2
 IDB 975 0 976 0
 Symbol -1 41 -2 -41

Functions: COMIS Function XMNCMI

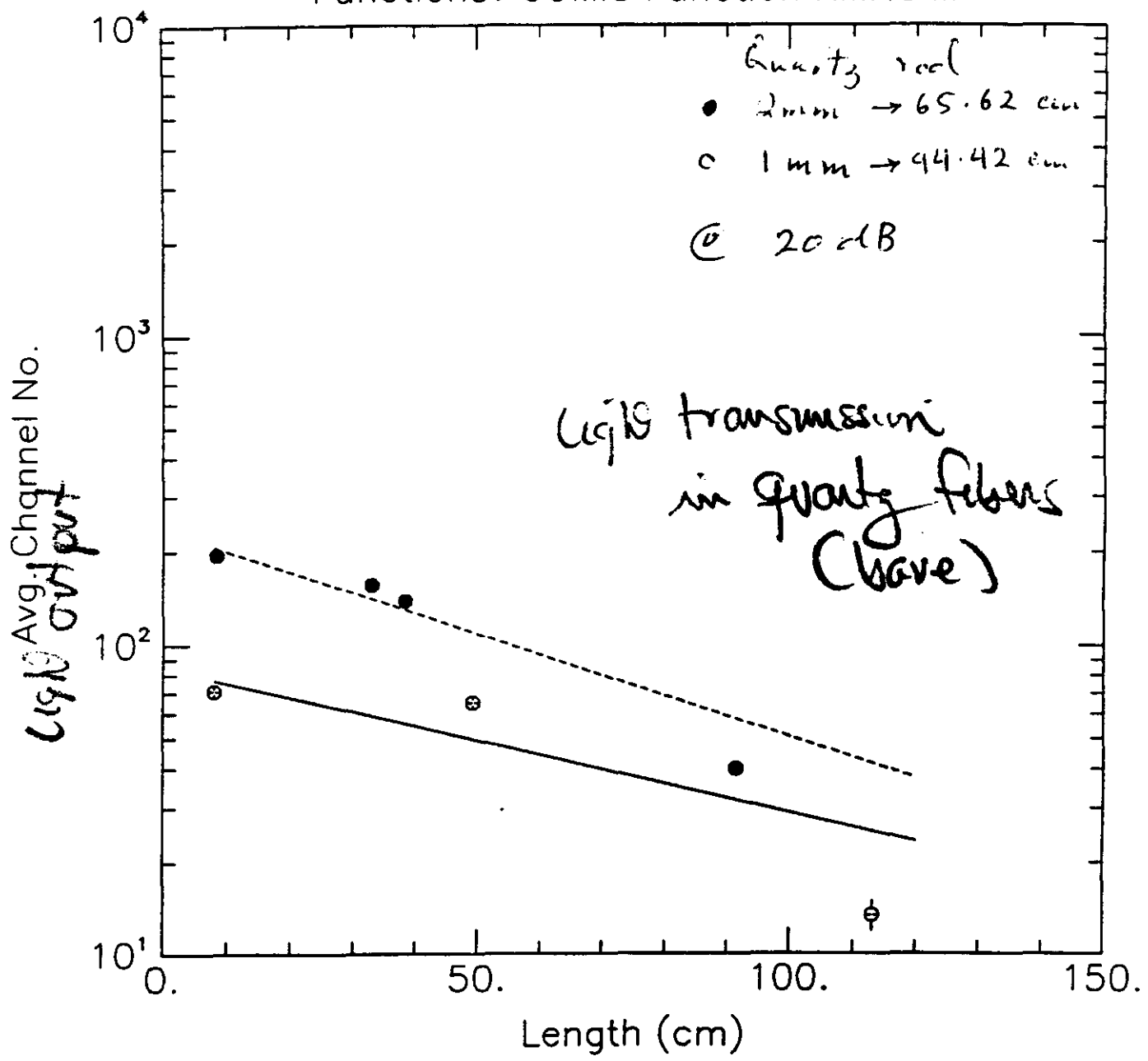


Figure 12

Quartz Monte Carlo Hadron Resolution (5% P.F; 4 m deep)

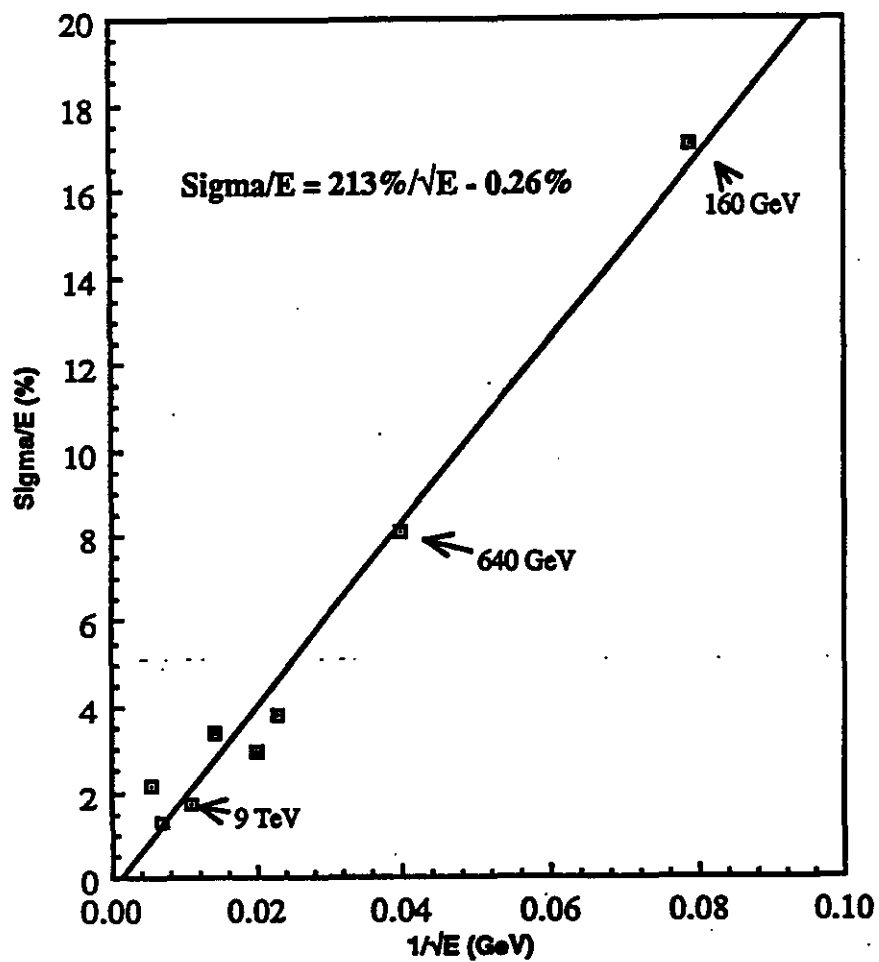


Figure 13

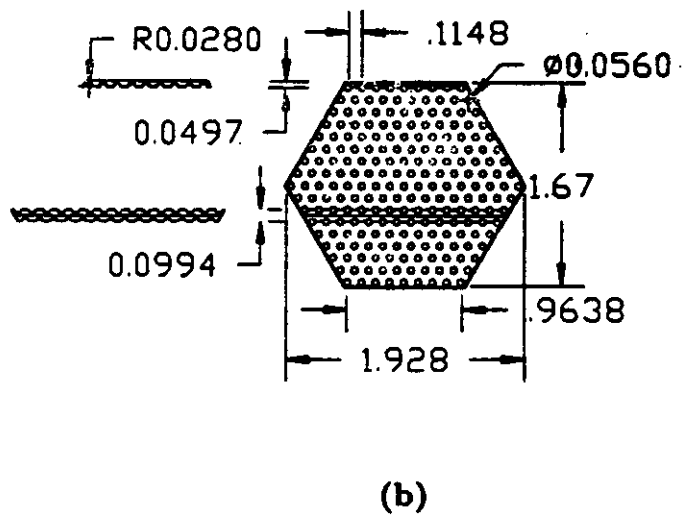
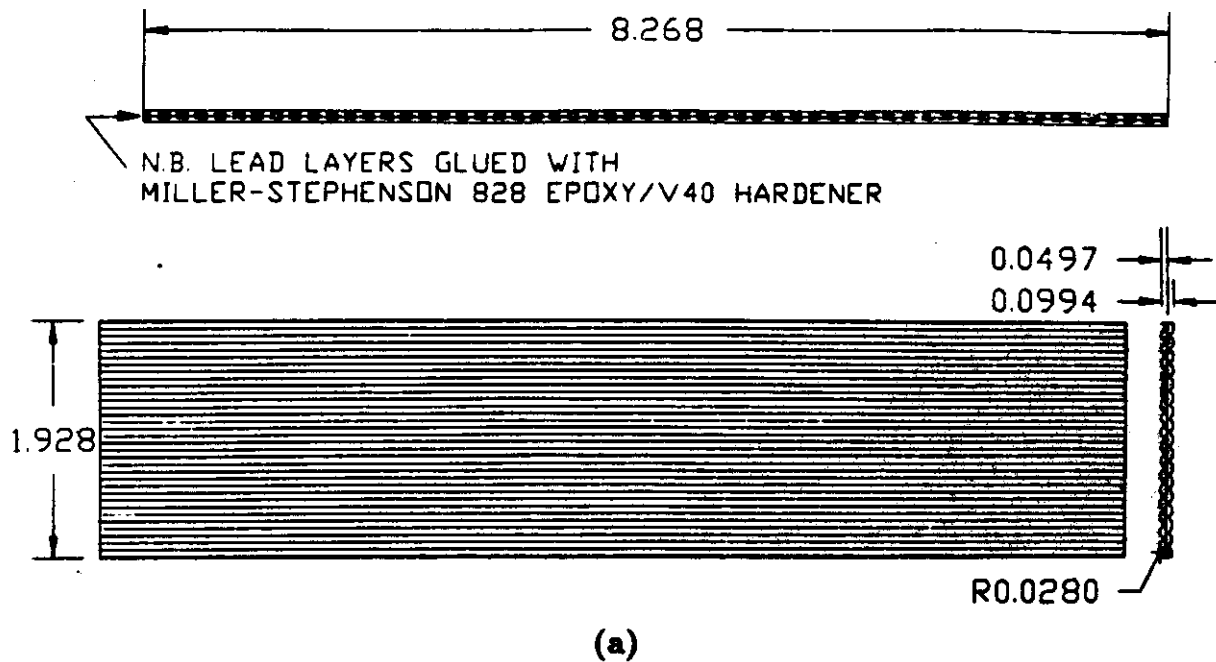
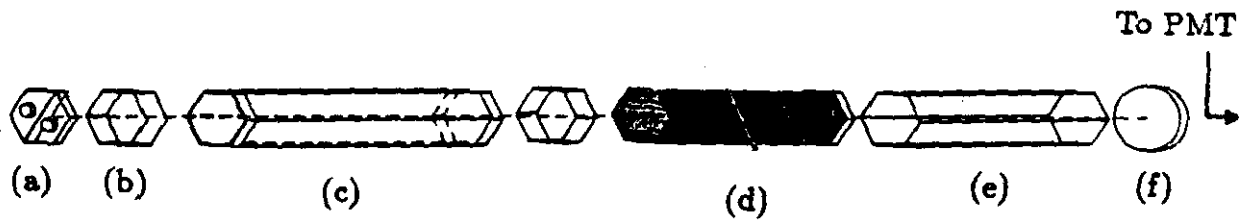


Figure 3. (a) Longitudinal & (b) End view of modules made from grooved lead plates (all dimensions in inches).

Figure 14



- (a) Hexagonal acrylic disk with tapped holes.
- (b) Stainless steel shim stock sleeve.
- (c) Hexagonal lead module.
- (d) Light guides.
- (e) Hexagonal UVT transmitting light collector.
- (f) Circular UVT transmitting acrylic disk.

Figure 7. Drawing a typical assembled module.

Figure 15

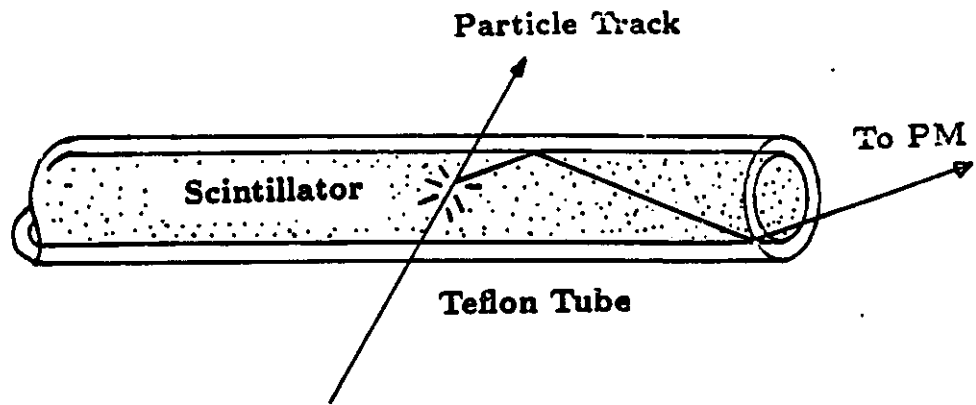


Figure 1. Diagram of a liquid scintillator filled Teflon tube.

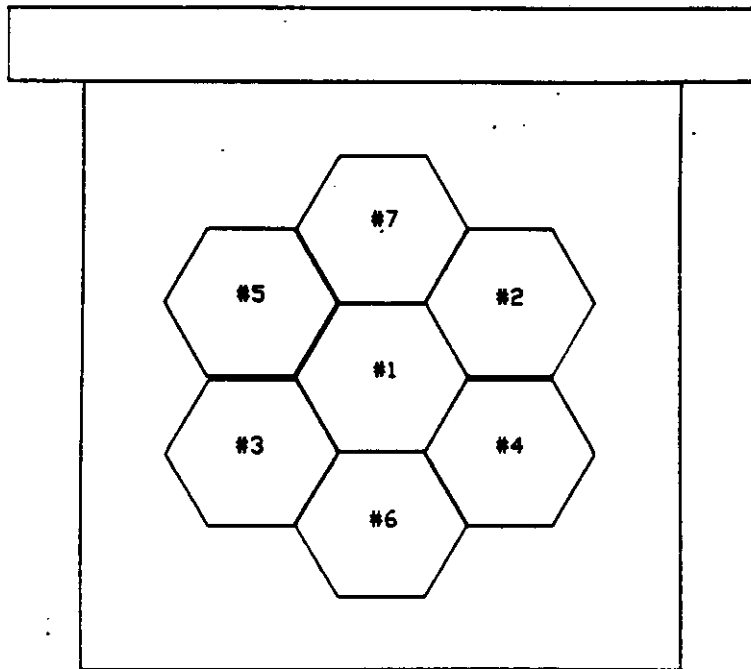
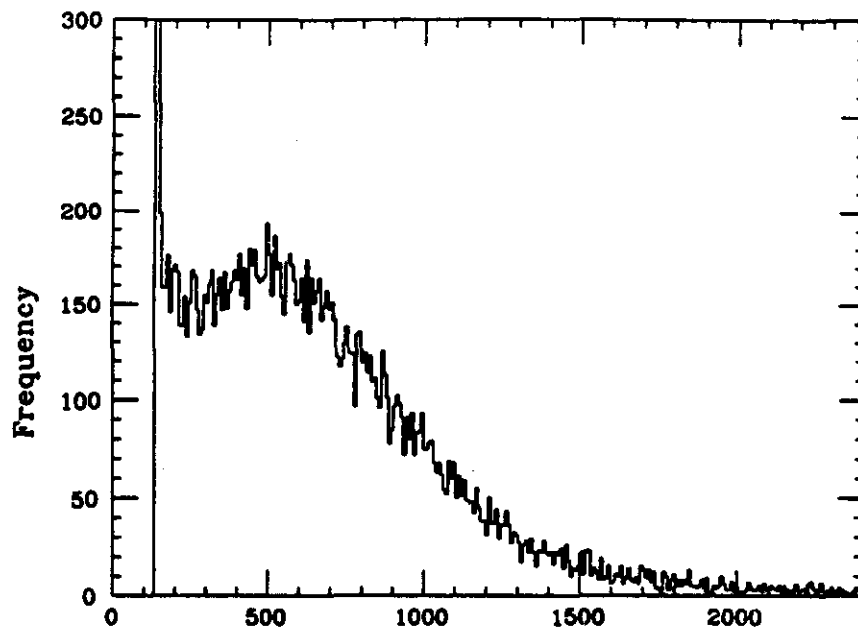


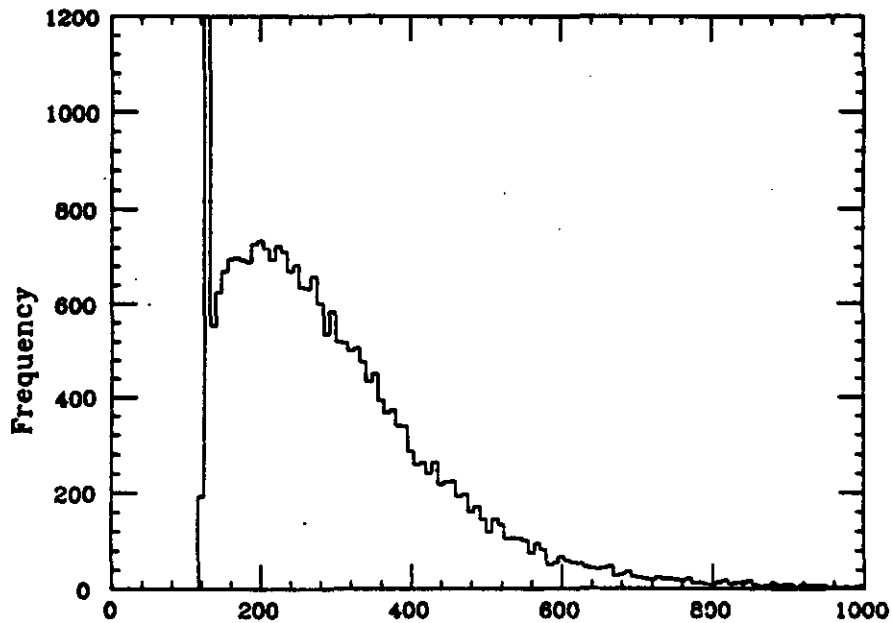
Figure 2. Cross section of lead modules in contiguous position.

Figure 1b



Counts (summed over modules)

(a)

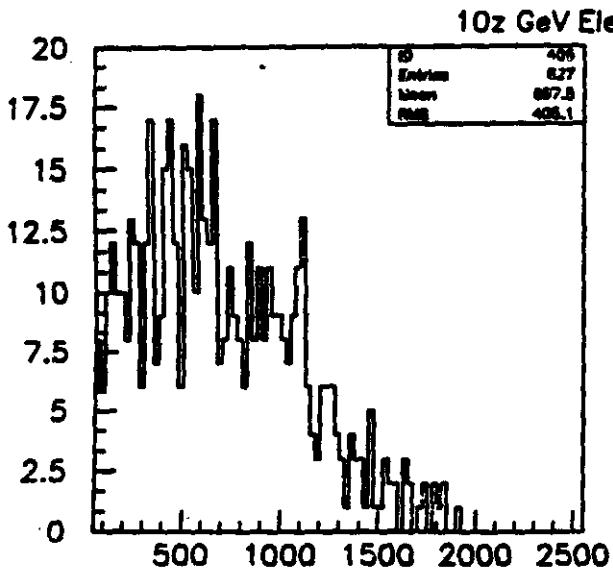


Counts (summed over modules)

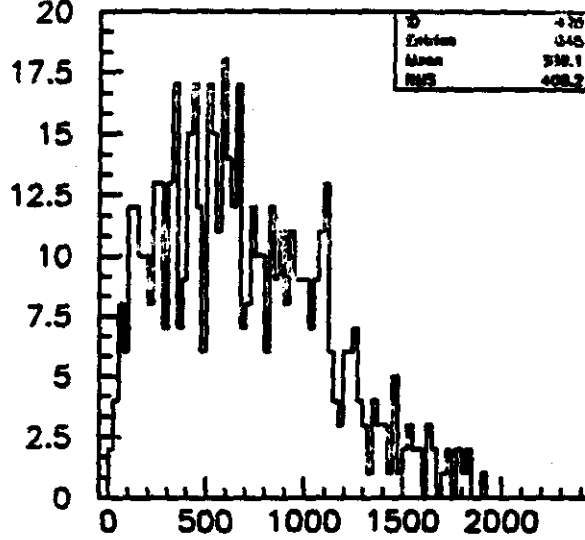
(b)

Figure 20. (a) Results of the front region summed over modules showing the 13 photoelectron spectrum. (b) Results of the back region summed over modules showing the 2.5 photoelectron spectrum.

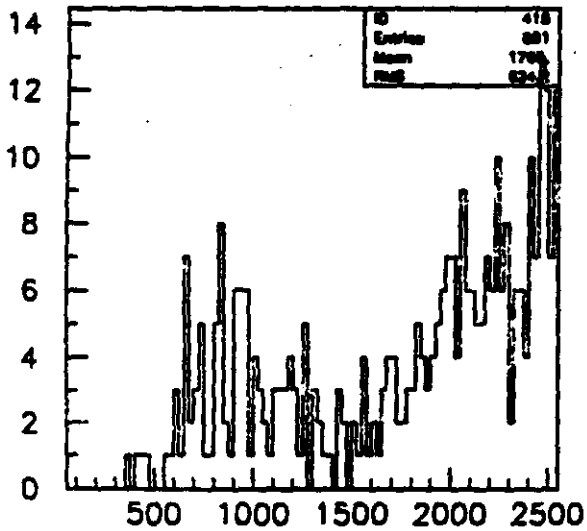
Figure 17



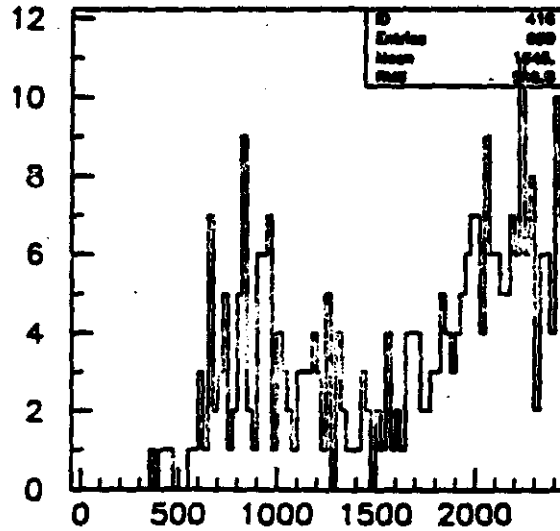
Module 5 ADC



Module 5 ADC



Sum all modules



Sum all modules

Figure 18
 Sample BNL pulse heights
 TAMU module

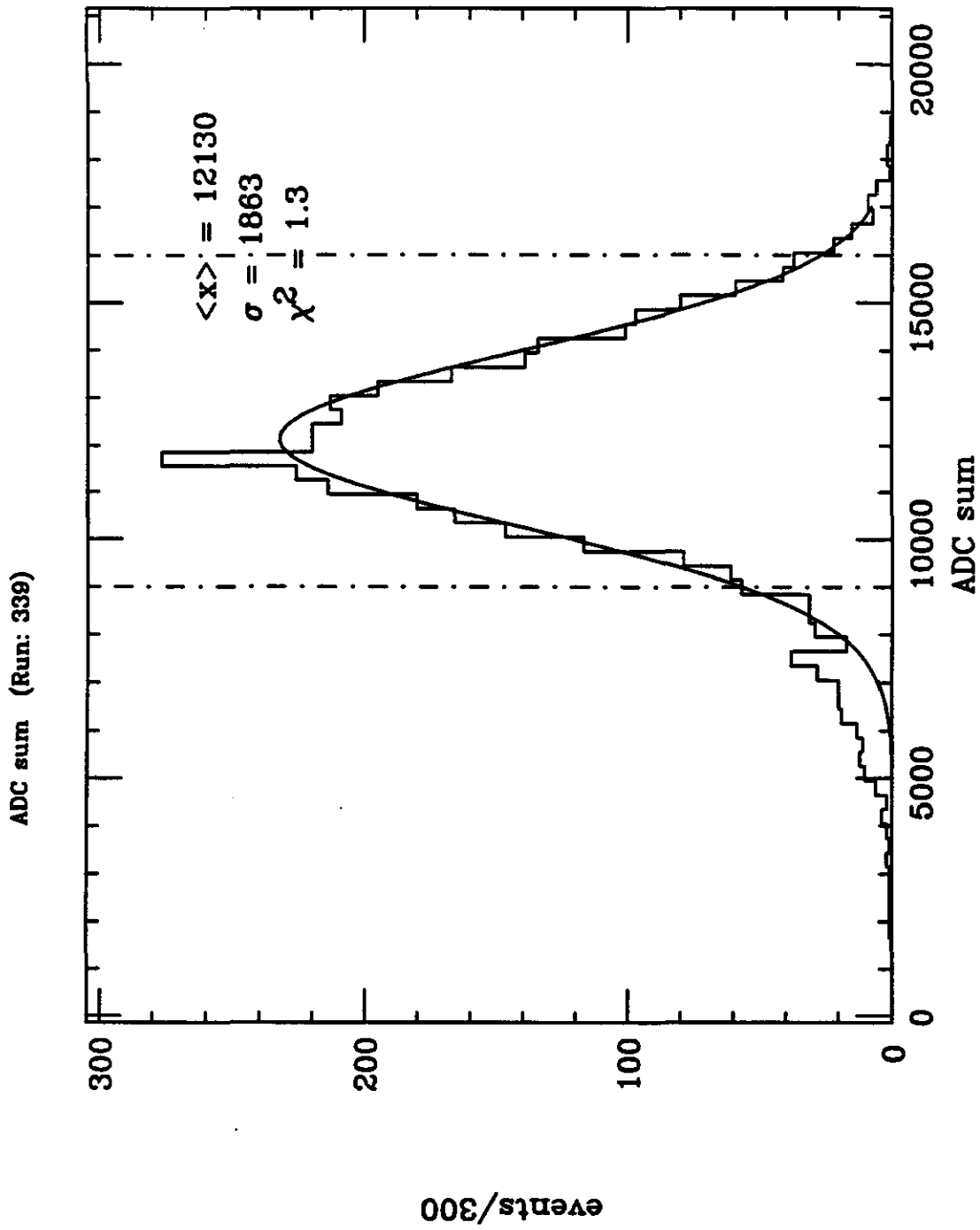
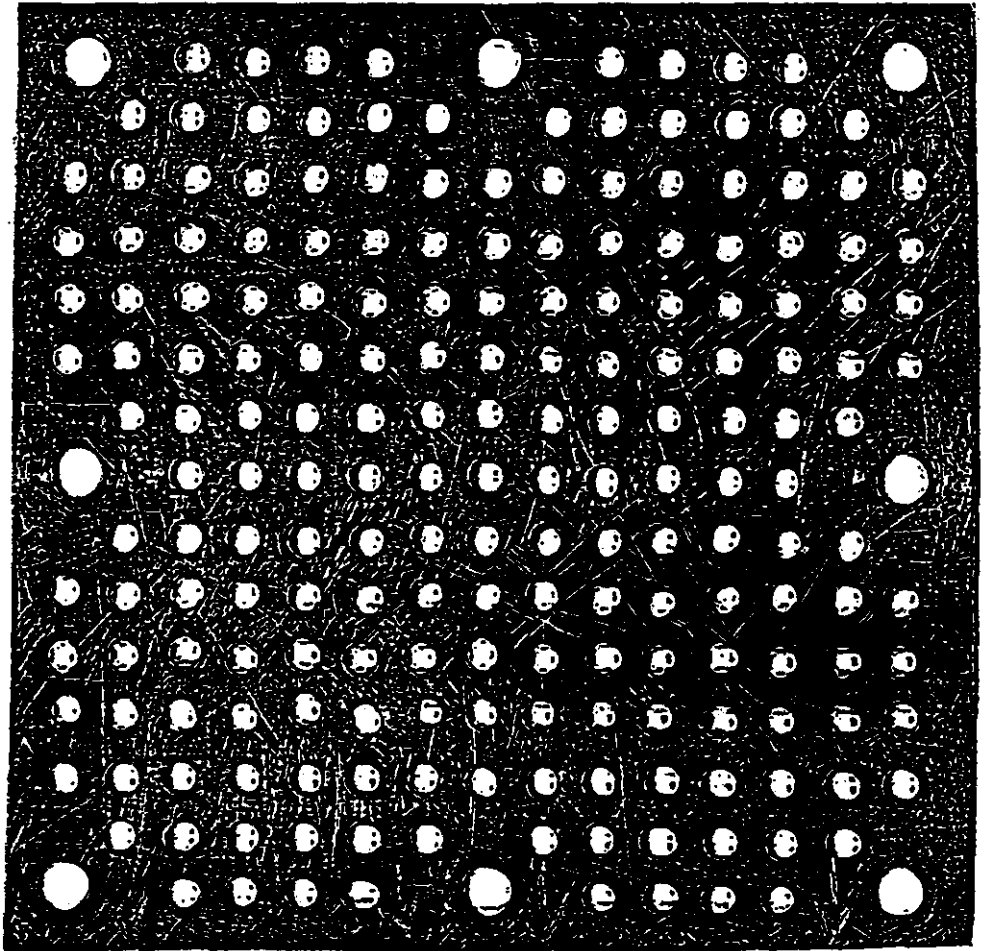


Figure 19

Fairfield Module.

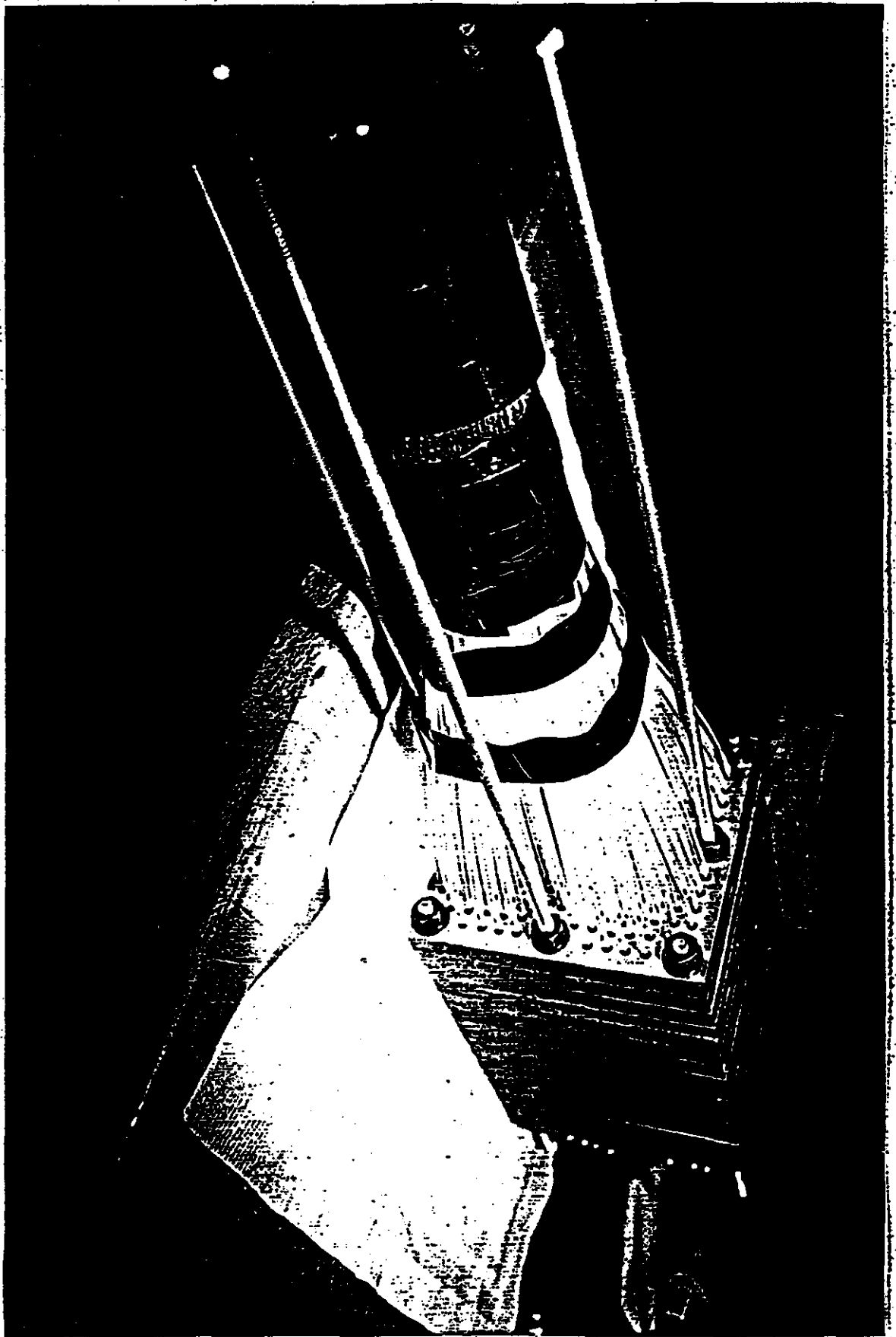


← 12.8 cm →

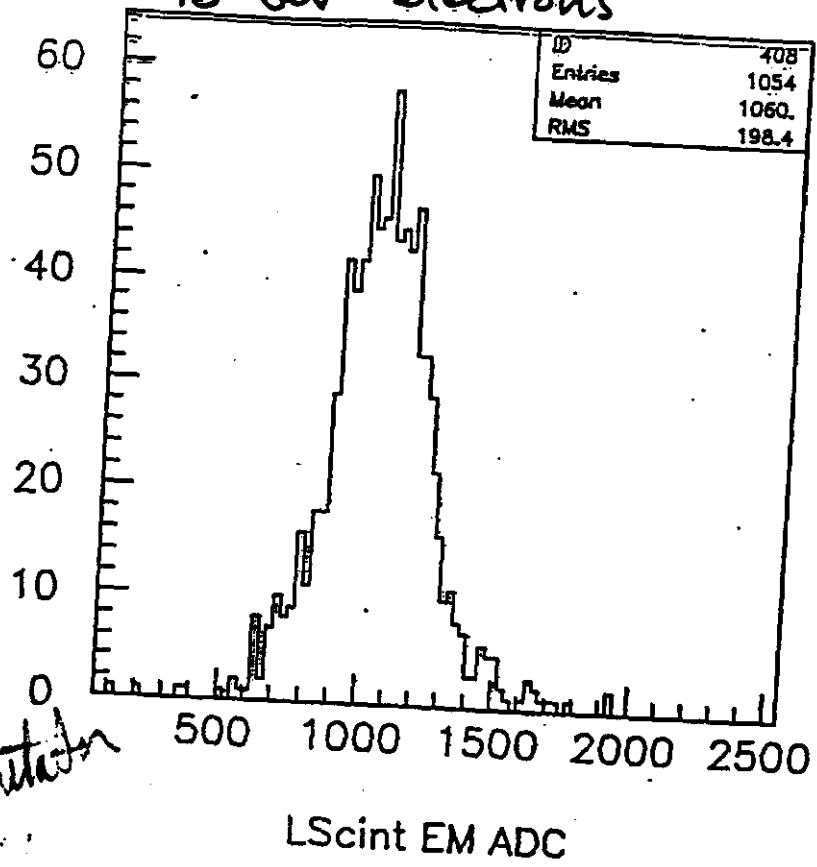
stole plate

Figure 20a

Figure 20b

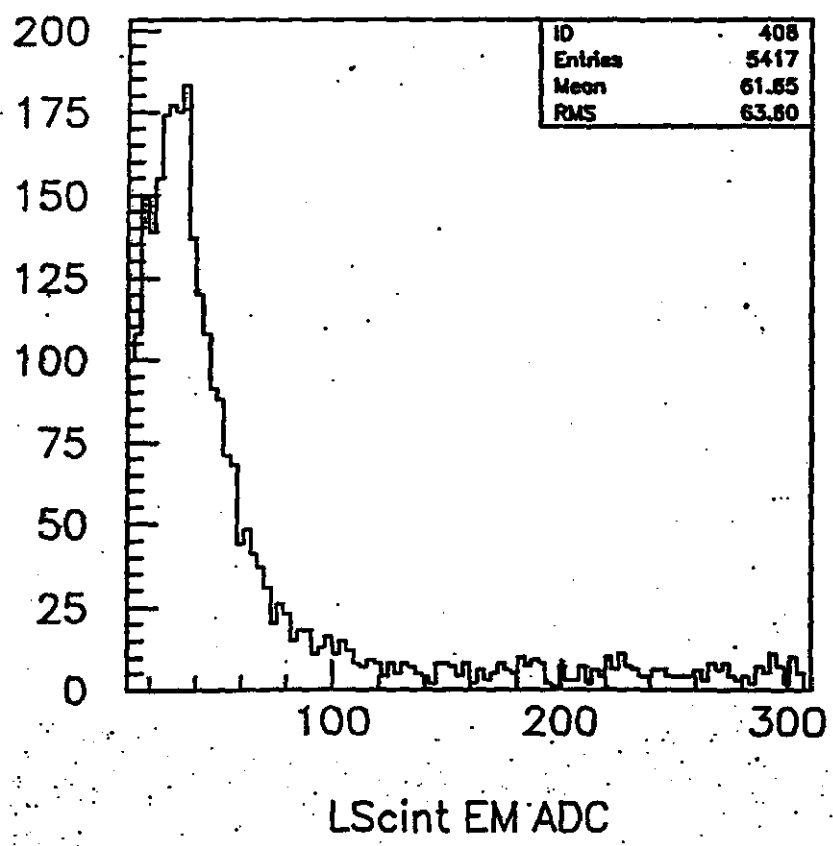


15 GeV electrons



Liquid Scintillation
Data
Fourfield

Figure 21.



1-Jan-89
8:28:22
Record
Traces

Liquid Scintillator

LeCroy

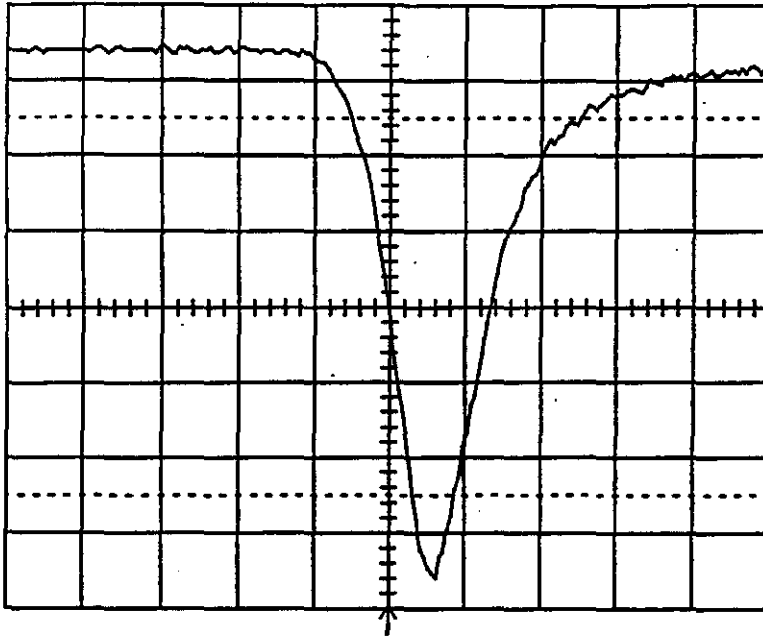
TRACE2.003
20 ns .2 V

Learn
Program

Turn On
XY Display

Turn On
Persistence

Configure
System



15 GeV e⁻

Figure 22

1-Jan-89
9:17:19
Record
Traces

Liquid Scintillator

LeCroy

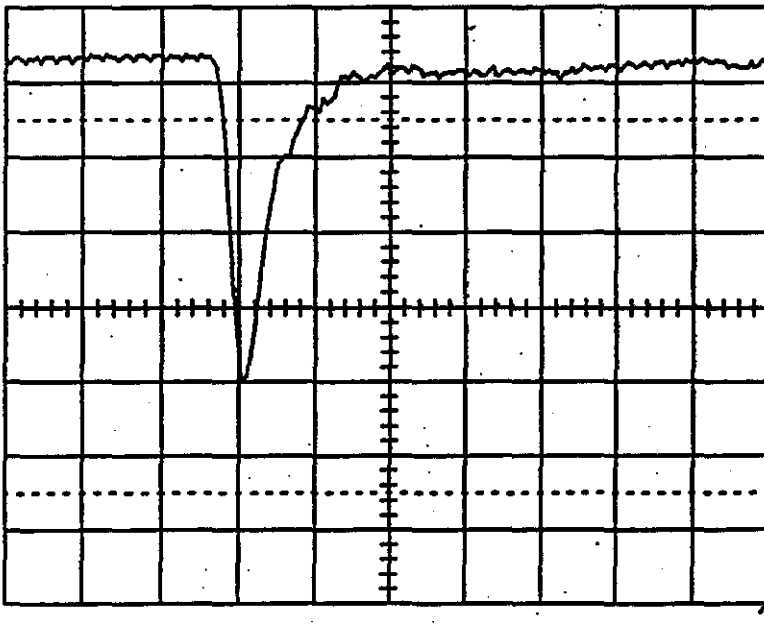
TRACE3.018
20 ns 20 mV

Learn
Program

Turn On
XY Display

Turn On
Persistence

Configure
System



15 GeV μ 's



Turn On
Multi Zoom

1-Jan-89
8:21:36
Record
Traces

Quartz fibers

LeCroy
⊕ TRACES.013
10 ns .5 V

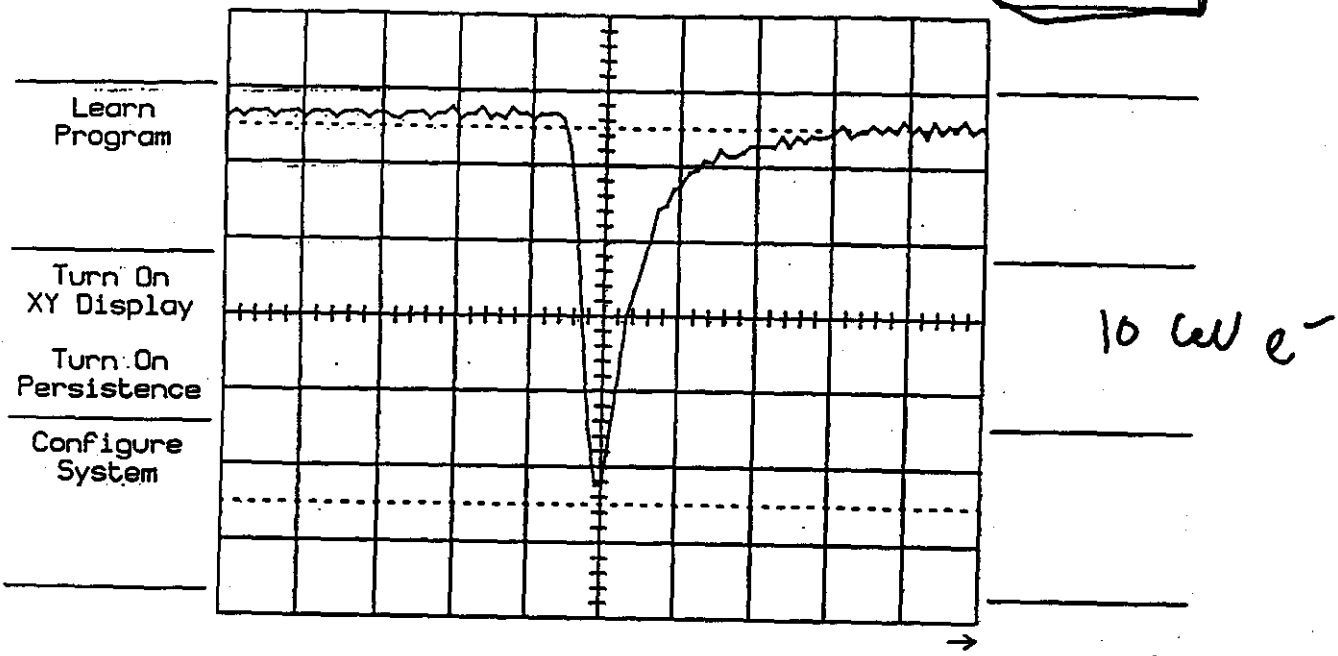
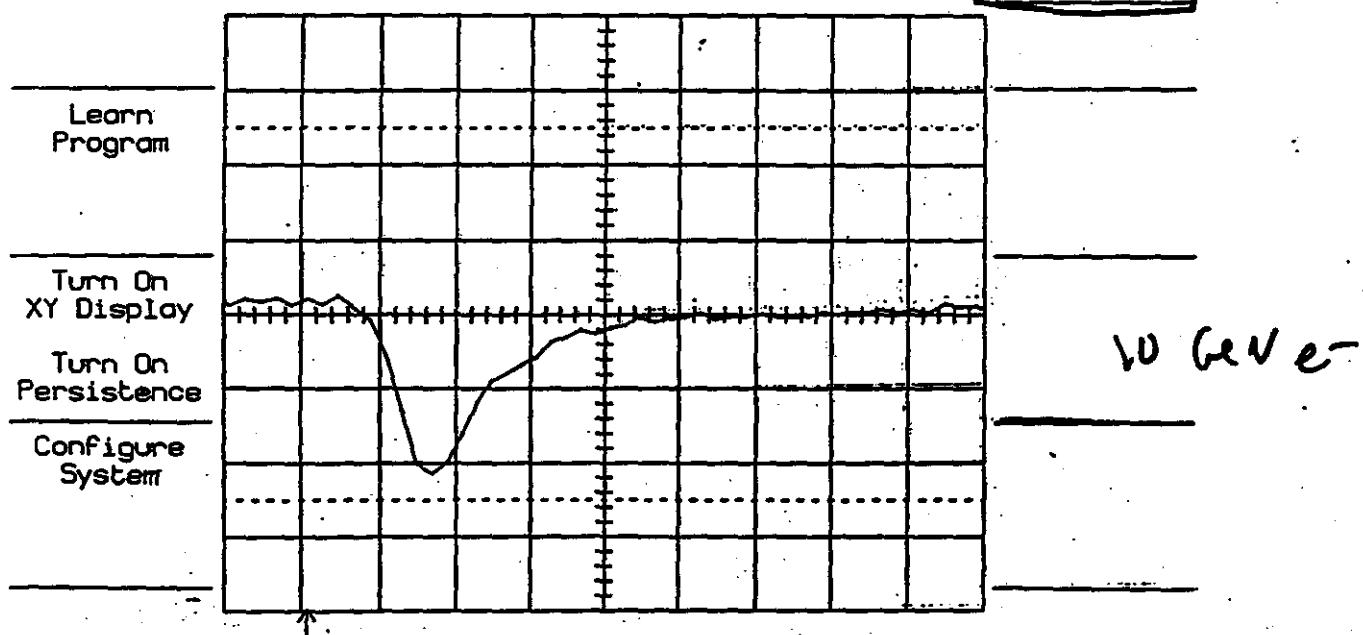


Figure 23

1-Jan-89
8:39:45
Record
Traces

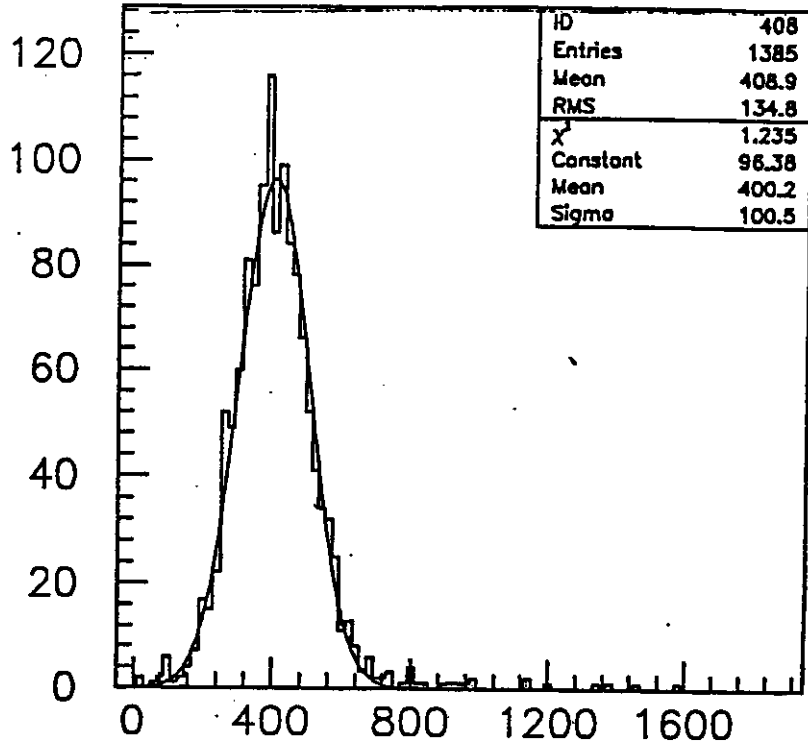
Quartz fibers

LeCroy
TRACES.023
5 ns 1 V



Turn On
Multi Zoom

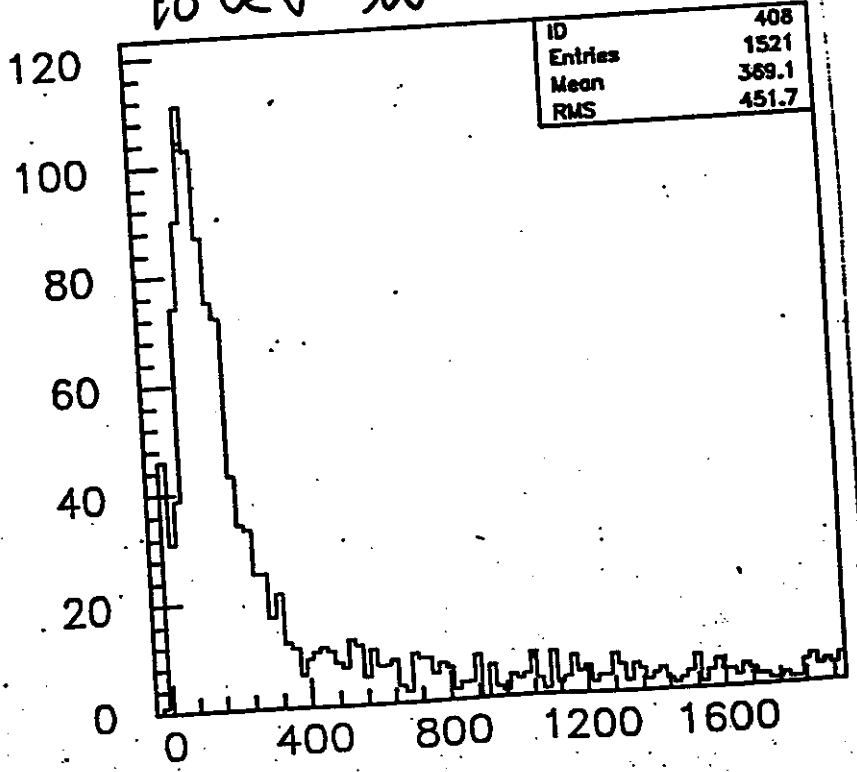
10 GeV e^-



Quartz Fiber
measurements

ADC ch
Figure 2f

10 GeV μ^-



ADC ch